Master of
Science Thesis
VT2017

NaCl pellets for improved dosimetry

Lovisa Walnder

Supervision

Christian Bernhardsson, Malmö

This work has been performed at
Medical Radiation Physics, Malmö

Department of Medical Radiation Physics,
Clinical Sciences, Lund
Lund University

Contents

Abstract

There is always a need to improve and develop new ways of estimating effective doses to people and environments that have been exposed to ionizing radiation. Dose monitoring is also important in hospitals and the nuclear industry.

Today there are several commercially available dosimeters, the most common being thermoluminescent dosimeters, TLDs, made from LiF. These are widely used for personal dose assessment in hospitals and in the nuclear industry but the LiF is expensive and the calibration is time consuming. Access to TLD's is usually limited and it would be desirable to develop a dosimeter that is readily accessible, easy to handle and cost effective on a large scale.

Salt has been shown to be sensitive to ionizing radiation and has been used in retrospective dosimetry. Because of the dosimetric properties of salt it has been investigated in this project if commercially available salt could also be used as a passive, prospective dosimeter. If this is possible the applications could include dose optimizations in hospitals, dose assessments after radiological or nuclear, RN, incidents, dose mapping of contaminated areas and dose estimations on an individual scale for people unintentionally exposed to ionizing radiation.

The aims of this project have been to find the optimal configuration for salt when pressed to the form of a pellet. Further, the dosimetric properties of the NaCl pellets, produced using six kinds of salt, have been investigated and a prototype dosimeter holder with appropriate energy compensation filters have been suggested.

This project has shown that NaCl pellets are best when produced using salt grain sizes between 100-400 μm and a compression force of 3.0±0.5 tons. Further, the readout protocol used to obtain the OSL signal, which has been used for many previous measurements on salt, has been altered in this project because it was found that heating the NaCl pellets changes the sensitivity. In the new readout protocol, there is no heating of the NaCl pellets.

The results also show that salt in the form of NaCl pellets have a linear dose response up to at least 6 Gy and that doses can be estimated using only one calibration, of the same size as the unknown dose, up to 100 mGy. For larger doses, >100 mGy, there is a sensitization of the pellets after exposure which complicates the dose estimations. The OLS signal show an inverse fading of about 20% after about 14 days when using the new readout protocol and the signal fading needs to be further investigated to obtain reliable results. Because of the low background signal in the NaCl pellets the MDD is very low, around 4-6 μGy, and it is possible to calculate an absorbed dose from the natural background after only three days.

The conclusions of this project are that stable NaCl pellets can easily be produced and they have dosimetric properties which are suitable for dosimetry. With the appropriate energy compensation filters the NaCl pellets could be used as simple and accessible dosimeters in both hospitals, the nuclear industry and for individual dose assessments.

Swedish popular summary (Populärvetenskaplig sammanfattning)

Det finns alltid en strävan att kunna uppskatta stråldoser på bättre och mer effektiva sätt. Om det så handlar om människor som blivit exponerade för joniserande strålning vid en olycka, ett attentat med radioaktiva ämnen eller för att mäta stråldoser på t ex. sjukhus. Idag finns det många kommersiellt tillgängliga alternativ för att utföra dosmätningar, så kallade dosimetrar. Samtidigt hade det varit önskvärt med alternativa dosimetrar som är mer tillgängliga, enklare att använda och som kan användas storskaligt på ett kostnadseffektivt vis.

I tidigare undersökningar har det visat sig att vanligt hushållssalt (NaCl) är känsligt för joniserande strålning och att det kan användas för att uppskatta stråldoser. När saltet bestrålas ackumuleras en signal som kan läsas ut med hjälp av en metod som kallas optisk stimulerad luminiscens, OSL. Salt har tidigare använts för att mäta stråldoser efter att en olycka har skett, dvs mätningarna har varit retrospektiva. Nu är tanken att saltet istället ska användas som en prospektiv dosimeter och för att förenkla hanteringen pressas saltet samman till små runda pellets. I prospektiva mätningar placeras dosimetern ut i förväg, innan strålningsexponeringen, på en plats eller en person för vilken man vill uppskatta en stråldos. Efter en tids mätning tas dosimetern till ett laboratorium där den ackumulerade signalen läses ut. Signalen kan räknas om till en stråldos som kan relateras till risker för både akuta och sena bieffekter på hälsan.

Med hjälp av en enkel och lättillgänglig dosimeter kan dosuppskattningar göras på individnivå, de kan användas för kartering av stora områden som blivit radioaktivt kontaminerade samt för dosreducerande dosmätningar på sjukhus mm. Den låga kostnaden för tillverkning och utläsning av de föreslagna saltdosimetrarna gör också att fler kan använda sig av metoden. I länder där strålskydd för personal och patienter inte prioriteras pga. begränsade resurser kan NaCl pellets användas för dosmätningar, och strålningsmiljön kan därmed bli säkrare för både personal och patienter.

Målet med detta projekt var att ta fram en saltdosimeter för noggranna mätningar av stråldos. Först undersöktes optimal konfiguration vad gäller kornstorlek och tryck för att forma salt till pellets. Vidare undersöktes de dosimetriska egenskaperna hos saltet i pelletform. Energikompenserande filter som används för att saltet ska kunna användas som en dosimeter har också undersökts.

Sex olika salter, varav fem finns tillgängliga hos alla stora svenska matvaruhus, undersöktes initialt för att utreda vilka typer av salt som ger bäst signal och tre av salten valdes ut för vidare undersökningar. Dosresponsen, signalminskning med tid och förändring i signalkänslighet efter bestrålning undersöktes. Det utläsningsprotokoll som används för att läsa ut signalen från saltet utvecklades också. Genom att pressa saltet till pellets förenklas hanterandet både vid mätningar och vid utläsning. De dosimetriska egenskaperna hos salterna är lovande vad gäller signalstabilitet, reproducerbarhet och dosrespons. Samtliga tre av de mest undersökta salterna är möjliga att använda i en dosimeter och som komplement eller ersättning till kommersiellt tillgängliga alternativ.

List of abbreviations

CW-OSL – Continuous Wave OSL

D_c – Calibration dose given to salt

D_u – Unknown or administered dose to salt

LED – Light Emitting Diode

MDD – Minimum Detectable Dose

NaCl – Sodium Chloride

OSL – Optically Stimulated Luminescence

OSLD – Optically Stimulated Luminescence Dosimeter

PMT – Photo Multiplier Tube

RN – Radiological and nuclear

SAR – Single Aliquot Regeneration

S_c – OSL signal resulting from readout after irradiation with D_c

S_u – OSL signal resulting from readout after irradiation with D_u

TL – Thermoluminescence

TLD – Thermoluminescence Dosimeter

1. Introduction

In the field of medical radiation physics there is always a need for improved and more effective ways of estimating absorbed and effective doses to people and in the environment. To consider the radiation protection workflow in terms of justification, optimization, and dose limits for procedures in e.g. hospitals and nuclear industry, there must be effective ways for dose assessments.

Today's most common commercially available dosimeter is the thermoluminescence dosimeter, TLD, usually LiF with various dopants (Kortov, 2007). The TLD's are rather expensive and the LiF is toxic. They can be used for both personal dose assessments and other dose measurements, like medical and radiobiological applications. Access to TLD's is often limited in hospitals for other purposes than personal dose assessments and the calibration process is time consuming. Another type of dosimeter used commercially is made from Al_2O_3, that is read out by optically stimulated luminescence, OSL. This dosimeter is patented and applications are limited. In addition to the already available dosimeters it would be desirable to develop a readily accessible dosimeter that is easy to handle in regard to calibration and readouts, and which enables accurate dose estimations in a cost-effective way, even on a large scale.

The current methods for estimating radiation doses from unintentional external exposure are bases on models in which location and occupation factors are considered together with (limited) point measurements and analyses of the contaminated areas. Usually, the main task of modelling is an assessment of the dose to a reference individual or group. Hence, these methods are associated with large uncertainties, because point measurements do not fully describe the varying radionuclide concentrations or radiation fields and the model cannot adopt fully to individual habits.

For external exposure, there are also other ways of estimating effective doses using retrospective methods. There are mathematical models that make use of Monte Carlo simulations based on point measurements and the method described in the previous section, biological methods and physical methods. Many biological methods have rather high detection limits which means that an individual might have to be exposed to rather high levels of radiation before accurate results can be obtained. Many of the methods are also rather complicated and require dedicated and expensive laboratories which are usually limited to major hospitals, as well as requiring special expertise. It is also uncertain in which capacity these methods can be implemented on a large scale in an emergency situation (Ainsbury et al., 2010).The physical methods also have limitations and in the case of OSL and TL these often depend on the properties of, and access to the materials(Mckeever and Moscovitch, 2003). One major drawback with materials used for OSL dosimetry is that the material must be kept shielded from light between exposure and readout to keep the stored signal.

Quarts and feldspar have luminescence properties that may be used for applications in optically stimulated luminescence (OSL), such as determine the age of an object (archeological dosimetry) or to estimate an absorbed dose in an object that has been exposed to ionizing radiation other than background radiation (retrospective dosimetry)(Bøtter-Jensen et al., 1996; Godfrey-Smith, 1994; Ramzaev et al., 2008). NaCl has also been shown to have OSL properties suitable for retrospective OSL dosimetry (Bernhardsson et al., 2009) and in theory, it would be possible to measure the total radiation exposure in a home in e.g.

Chernobyl contaminated villages in Russia and Belarus since the accident by performing OSL measurements on salt taken from someone's kitchen cabinet. Since the signal of OSL materials is light sensitive and it cannot be assured that the salt has been kept from light between exposure and readout, the retrospective dose assessments in NaCl have large uncertainties (that increase with the time after exposure when sampled from a kitchen cabinet).

However, since previous works on retrospective applications have shown that the salt is highly sensitive to ionizing radiation (Bernhardsson et al., 2009), it would be possible to, instead of using the salt as a retrospective dosimeter, use it as a passive, prospective dosimeter. Salt is cheap, easily accessible and the method for dose estimations is rather simple. This together with a linear dose response and low fading makes salt suitable for prospective dosimetry. Even more so if the handling and reproducibility can be improved. In this project, a method is suggested where the salt is pressed into pellets making the salt more homogeneous and easier to handle.

The suggested production method of making dosimeters made from salt enables mass production and distribution, both for individual dose assessments of the public and for more detailed dose mapping of large areas which have been exposed to ionizing radiation. Other applications for the NaCl dosimeters can be found in hospitals and in nuclear industry. They can also be used for personal dose monitoring and in other dose measurements where, for example, TLDs, Al_2O_3 or dosimetric films are used today. In some countries where the radiation protection is not prioritized because of limited resources the suggested dosimeter could potentially provide for new improvements in terms of dose optimization in hospitals and other areas.

After the nuclear accidents in for example Chernobyl (USSR, 1986) or Fukushima (Japan, 2011), large areas were contaminated by fallout and there was a need to determine the radiation doses to the people living in the affected areas. In these situations, large groups of people, in many cases whole villages or settlements, may be forced to evacuate due to the high levels of exposure. In some areas the evacuation is voluntary but many people choose to evacuate because of anxiety of the radiation (Murakami et al., 2015). However, in the case of the Fukushima accident the evacuation led to increased mortality rates and increased severe psychological distress among the evacuees (Kunii et al., 2016),(Murakami et al., 2015). If the dose assessments could be improved, some of the people that evacuated due to anxiety based on results from today's methods, might potentially choose to stay in their homes, without a significantly increased risk of cancer development later in life.

To fully use the potential of the NaCl dosimeter, a readout unit is necessary. The description of a simplified OSL readout unit is beyond the scope of the present project, but little efforts would be needed to build such a device, which would further improve the usability of the suggested dosimeter.

The specific aims of this thesis are:

- To find the optimal configuration for pressing and forming a pellet of NaCl which can be used as a dosimeter.
- To investigate the dosimetric properties of NaCl when in the form of pellets.

- Suggest a prototype of a dosimeter holder with appropriate energy compensation filters for the NaCl pellets in various areas of application.

1.1 Retrospective Dosimetry

Retrospective OSL dosimetry is used mainly in archeological dating and accident dosimetry (unintentionally exposed individuals). The methods used to obtain the absorbed dose in the materials are the same in both cases, the difference is the origin of the dose to be estimated: natural background radiation or exposure from anthropogenic radionuclides.

In dating applications, the absorbed dose in a material is determined to calculate the age. The material has been exposed to ionizing radiation from radionuclides of the uranium and thorium series in the ground and from cosmic radiation mainly. By measuring the surrounding dose rate, where the material was sampled, and the absorbed dose in the material an age can be calculated.

A luminescent material can be reset, zeroed, by the use of heat or light. Materials that are zeroed by light must be kept in the dark to keep the stored energy. For dating this means that the age is determined from the time the material was last zeroed, that is, the last time it was exposed to high temperatures or daylight. For example, a ceramic pot was zeroed when it was fired and if later hidden in sediments or layers in the ground it was last zeroed when it was latest exposed to daylight (Thomsen, 2004).

In connection with a radiological or nuclear (RN) accident or an act of terrorism involving RN materials it is important to be able to estimate the exposure of the population and the emergency responders, preferably on an individual level. In emergency dosimetry, an absorbed dose is determined in materials after an unexpected event involving ionizing radiation. In the early phases after an accident the results obtained from retrospective dosimetry methods can be used for triage, treatments and to focus resources to where they are needed most (support for decision making). The dosimetric data can also be used to calm and inform the public, reconstruct individual doses, assess long term effects as well as for epidemiology.

The signal used to estimate the absorbed dose can be obtained from minerals in for example, bricks, porcelain, electronic components or dental ceramics (Thomsen, 2004). The minerals used in OSL applications are usually quartz, feldspar or Al_2O_3.

1.2 Luminescence

Band Theory

Around the nucleus of an atom, electrons orbit in fixed energy states. When a molecule is formed by two atoms the energy states overlap but since two electrons cannot have the same quantum number in a solid according to the Pauli principle, the atomic orbits will split up and form two molecular orbits. In a crystal structure the electron orbits split up into many molecular orbits, forming continuums of energy states called energy bands. In the ground state of the crystal the electrons start to fill the energy states starting with the lowest energies. The highest filled energy band is called the valence band and the lowest empty energy band is called the conduction band. The conduction band is the lowest band of unoccupied energy state and electrons that occupy it can freely move around in the solid, assuming a perfect lattice. Between the valence and conduction bands, in a perfect crystal lattice, there is a gap in

which no charges are allowed. In conducting materials, the band gap is small or non-existent, whereas, in insulators the band gap is large and in semiconductors the band gap is of intermediate size. In insulators, the energy gap is greater than 2.5 eV and electrons cannot be excited from the valence band to the conduction band by thermal vibrations at room temperature.

In reality, the crystal lattice is not perfect and there are defects caused by impurities within it. The impurities cause local electric fields which can capture free electrons from the conduction band. The impurities are vacancies or foreign atoms in the crystal structure which interrupts the periodicity. These impurities and their local electric field give rise to energy states in the forbidden band gap. Impurity states that can trap charge carriers and re-emit them to where they came from are classified as traps. If the energy state on the other hand can capture charge carriers of opposite signs which leads to recombination, the energy states are called recombination centers.

The energy depth of a trap is defined by the difference between the energy of the conduction band and the energy of the trap state, since transitions to the valence band are forbidden. For a trap to be stable it must be deep enough not to be emptied by lattice vibrations. A charge in a stable trap can only escape if enough energy is supplied to promote it to the conduction band.

Luminescence

Materials with luminescent properties are crystalline and when exposed to ionizing radiation they may store some of the energy by redistributing the charge in the crystal. Some of the charge become trapped at defects in the crystal. The energy stored as trapped charge can be released by applying either heat or light. In the subsequent process the energy is released as luminescence that can be detected and measured in a laboratory.

The difference in energy between the conduction and valence band correspond to the minimum energy which must be absorbed by an electron for an excitation to take place. For insulators, electron transitions to the conduction band from the valence band are negligible without external energy. When ionizing radiation incident on the insulator it can interact with electrons and deposit enough energy to excite the electrons to the conduction band, leaving a hole in the valence band. Other electrons can then shuffle, causing the hole to move. The electron in the conduction band will in most cases de-excite, recombine with a hole and emit a photon with an energy matching the energy gap between the conduction band and the valence band or recombination center. This process is called fluorescence.

In some cases, the electrons get trapped in an energy state in the band gap, caused by impurities, in which it cannot spontaneously de-excite. For the electron to de-excite from such a state to the ground state it must first be re-excited up to the conduction band. After that it can de-excite and emit a photon with an energy matching the energy gap. This process is called phosphorescence.

Thermoluminescence

When stimulating a crystal lattice with ionizing radiation and promoting electrons to the conduction band, some of the electrons will be trapped at trapping centers. By de-trapping the electrons and measuring the resulting emitted photons (luminescence) it is possible to

estimate the absorbed dose to the material. In TL, the traps are emptied by rising the temperature of the material. In that process, energy is transferred thermally, and at certain temperatures enough energy is transferred for the electrons to re-excite to the conduction band before finding a recombination center. Different types of traps are emptied at different temperatures and when the electrons recombine with a hole in a recombination center the recombination center de-excites and a photon is emitted. When measuring the intensity of this light, in relation to the temperature, a glow curve is formed (right frame in Fig. 1). Since materials often contain different kinds of impurities there will be different kinds of traps, corresponding to different energies. This results in a glow curve with several peaks at different temperatures. The lifetime of electrons in traps depend on the energy of the trap, with longer lifetimes for deeper traps. The lifetime is also effected by quantum mechanical tunneling since charges can tunnel to other traps. More shallow traps, which can be emptied with temperatures below 200˚ are usually considered to be too unstable to be reliable for dosimetry purposes.

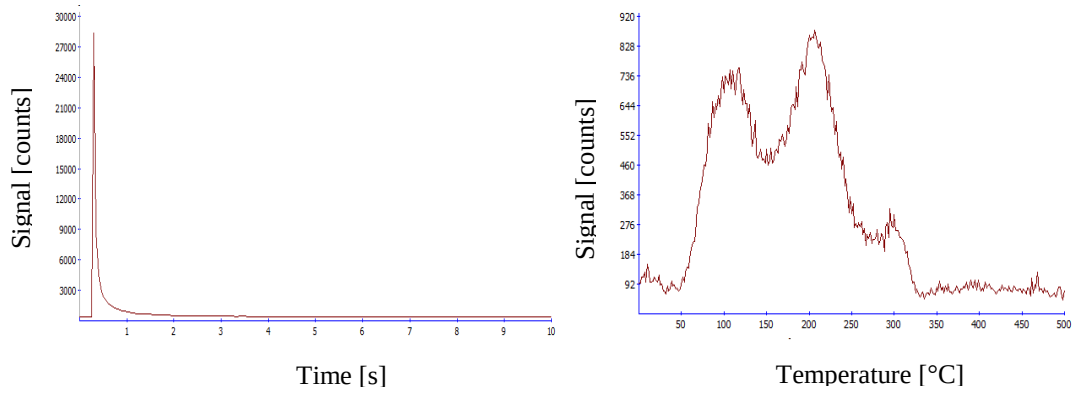

Figure 1. The graphs show typical glow curves when stimulating irradiated NaCl with light (left frame) and heat (right frame), respectively.

Dosimeters based on thermoluminescence are calibrated in a well-known beam, for example ^{60}Co or ^{137}Cs. The TLDs are irradiated at well-defined absorbed doses in the beam, and the absorbed dose is increased with every irradiation or alternatively, one fixed dose is delivered several times until a stable response is achieved. After irradiation, the TL signal from the TLDs are measured by a dedicated reader and then heated in an oven to completely empty the signal and restore the material. The relation between the TL-signals for the corresponding absorbed doses gives a calibration curve for each individual TLD. Hence, the calibration procedure of TL-based dosimeters is complicated and time consuming. After calibration, the TLDs are used several times before they are re-calibrated and it is assumed that the calibration is correct even with repeated usage. This introduces uncertainties unless the LiF chip calibraitons are verified between usages, for example by administering a small calibration dose after the known signal has been read out.

Optically Stimulated Luminescence

The concept of OSL is similar to that of TL but instead of depleting the traps with heat, light (photons) is used. The most commonly used stimulation mode in OSL is the so-called continuous wave mode, CW-OSL, where the intensity of the stimulating light is constant and the light emission, i.e. luminescence, is measured during the entire stimulation. Inside the reader, at the photomultiplier tube (PMT), filters are used to distinguish the luminescence

from reflected stimulation light. In CW-OSL, the intensity of the signal decreases with time of stimulation until the traps are completely emptied (left frame in Fig 1).

As previously mentioned, to reset the signal of the material to zero either heat or light can be used. This also means that for the material to store the signal it must be kept in the dark (at normal ambient conditions). It is possible that different traps are emptied using the different methods.

In the simplest OSL model it can be shown that the signal decays exponentially with time when the traps are emptied. If *n* is the number of trapped electrons in the traps and *p* is the probability of electron escape to the conduction band per unit time, *n* will change according to

$$\frac{dn}{dt} = -np \tag{1}$$

if the re-trapping is negligible. Solving Eq. 1 gives

$$n(t) = n_0 e^{-pt} \tag{2}$$

Assuming all holes and electrons recombine without delay, the light emitted is proportional to the amount of released electrons

$$I_{OSL} \propto \left|\frac{dn}{dt}\right| = n_0 e^{-pt} \tag{3}$$

The probability *p* depends on the wavelength and intensity of the stimulation light, a higher intensity gives a higher probability of de-trapping.

Trying to mathematically describe the OSL (or TL) process is very complex but with some simplifications the resulting equations can be used to describe several phenomena. The equations are non-linear differential equations which describe the rate of electron transitions between energy levels in a crystal. To solve the equations, it is assumed that charge recombination occurs by charge transport between the energy levels and that the system is in quasi-equilibrium which means that the processes are slow and the amount of charges in the valence and conduction band are small (Yukihara and Mckeever, 2011).

2. Materials and Method

2.1 Salt

Sodium Chloride, NaCl, is an alkali halide with a crystal structure. NaCl has a band gap of about 7 eV, making it an insulator. This means that the conduction band contains few electrons since the thermal energy of the electrons is not enough to excite them from the valence band to the conduction band. It has previously been shown that NaCl can be used in dosimetry for both thermoluminescence, TL, and optically stimulated luminescence, OSL (Bernhardsson et al., 2009).

In this project six different salts were used (Table 1), five of which can be found in ordinary Swedish supermarkets. Four of the salts were from the same brand, Falksalt (Ab Hansson & Möhring, Göteborg), but their composition or origin differ. The salt referred to as Falksalt 1 is a Himalayan salt, the one referred to as Falksalt 2 is a fine salt without added iodine, the one

referred to as Falksalt 3 is a fine salt with added iodine and the one referred to as Falksalt 4 is an ocean salt. Chemically pure salt from Scharlau (Scharlau Chemicals, Spain) and fine household salt from Jozo (Akzo Nobel, Sweden) were also used. More information about the salts can be found in Table 1 and the containers of the various salts are shown in Figure 2.

Table 1. General information about the various salts used in this project.

Name in text	Brand	Name	Production date	Best Before	Anti-caking agent/Iodine
Falksalt 1	Falksalt	Himalayasalt	2016-11-15	2019-01-02	No/No
Falksalt 2	Falksalt	Hushållssalt utan jod	2016-12-19	N/A	Yes/No
Falksalt 3	Falksalt	Hushållssalt med jod	N/A	2019-02-01	Yes/Yes
Falksalt 4	Falksalt	Medelhavssalt	2017-01-02	N/A	Yes/No
Scharlau	Scharlau	(Chemically pure)	N/A	2026-09-01	No/No
Jozo	Jozo	Fint salt med jod	N/A	2018-11-04	Yes/Yes

Figure 2. The original plastic containers of the salt used in the project. From the left: Falksalt 1, Falksalt 2, Falksalt 3, Falksalt 4, Scharlau, Jozo.

The graphs of Figure 3 show the various salts compositions in regard to grain size distribution in the packages.

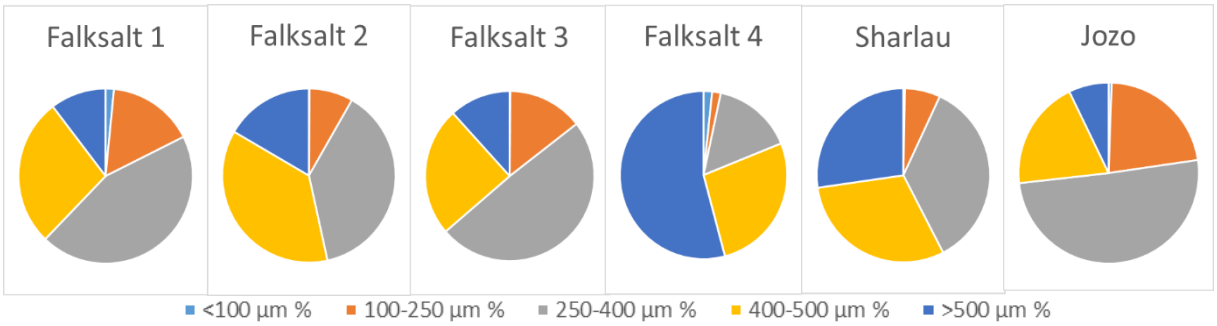

Figure 3. Grain size distribution of the different salts (Table 1) divided by fraction from <100 µm up to > 500 µm, in terms of % of the total contents in each container.

Salt in its original form, but sieved into different gran size fractions, was used to press pellets to increase the density and homogeneity of the dosimeter and to improve the process of operating them during exposure and readout. The pellets were pressed using a metal tool that has been specially developed for this purpose. The different parts of the tool are presented in Figure 4: salt is placed in circular cavities in the base of the tool (1), a lid with corresponding

rods is placed on top it (2), and a hydraulic press (3) is used to form the pellets with, by pressing part (1) and (2) together with salt in between, using 3 tons of compression force. The resulting NaCl pellets (5) are subsequently removed from the tool cavities with a separate tool (4) and put aside to rest for a few hours before they are used. The resulting pellets are 4 mm in diameter and about 1 mm thick. The details of how to make the NaCl pellets are given i Appendix A.

(1) (2) (3) (4) (5)

Figure 4. The different parts of the tool which is used to make the NaCl pellets. The salt is placed in the middle cavities of part 1, part 2 is put on top of it and the unit is put under a hydraulic press. Part 4 is used to remove the pellets from part 1. Image 5 shows the final pellets.

2.2 Risø TL/OSL reader

Throughout the current project a commercially available readout unit from DTU, Risø, Denmark, was used. The main components of this Risø TL/OSL (TL-DA-15) reader are the heater plate for individual heating of the samples, the irradiation source (Sr-90/Y-90), the stimulation light, and the photomultiplier tube (PMT) that collects the signal (luminescence). The samples are put on individual cups and placed on a carousel which can fit up to 48 samples. The Risø TL/OSL reader can stimulate the samples in both TL and OSL mode.

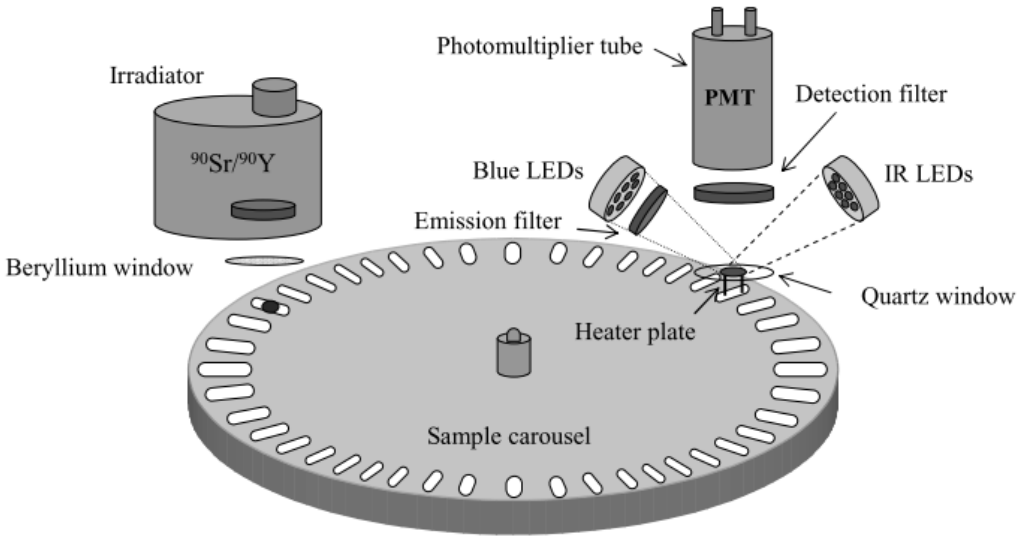

Figure 5. The figure illustrates the main internal components of the Risø OSL reader (Thomsen, 2004).

The reader can heat the samples up to 700 ˚C at different heat rates using a heating element made from the alloy kanthal (iron, chromium and aluminum). To assure that the heat is properly transferred to the sample, it is recommended to use low heat rates around 2-10 °C/s. Nitrogen gas, N_2, is used to cool down the heating element. The heating element also works as

the lift that places the sample at the signal acquisition position close to the PMT. The element is heated by a current produced by a 20-kHz sine wave generator.

The stimulation light is used to release the stored luminescence after exposure to ionizing radiation i.e. empty the traps. The probability for a trap to be emptied depends both on the number of photons that interact with it and the wavelength of the stimulation light. A shorter wavelength (higher energy) gives a higher probability of emptying the trap. It should be noted, that the current mode of the readout unit is dedicated for measurements on Quartz. It has two options of light stimulation (OSL), either red LEDs or blue LEDs. It has previously been shown that the optimal light stimulation source of this unit is the blue LED (λ=470±30 nm), when using NaCl as OSL material (Christiansson, 2014).

For the PMT to only be exposed to the luminescence light and not scattered stimulating light, a filter combination is used. The filters are important since the stimulating light is around 10^{18} orders of magnitude larger than the luminescence (Thomsen, 2004). To achieve the optimal detection, the spectral windows of the stimulation and the luminescence light must be well separated. The Risø reader uses a GG-420 longpass emission filter in front of the blue LEDs in combination with a 7.5 mm thick Hoya U-340 detection filter in front of the PMT which reduces scatter from the LEDs.

2.3 Readout Protocol

The standard readout protocol, previously developed at the Medical Radiation Physics group in Malmö, Lund University (Bernhardsson et al., 2009) is as follows:

- Unknown dose or given dose, D_u (mGy)
- Preheat at 220 ˚C with a heating rate of 10 ˚C/s and maintained for 10 seconds
- Readout of OSL at 100 ˚C with a heating rate of 5 ˚C/s using blue LED at 40 % of the maximum intensity. Resulting in signal S_u (counts)
- Calibration Dose, D_c (mGy) using the internal ^{90}Sr/^{90}Y beta source
- Preheat at 220 ˚C with a heating rate of 10 ˚C/s, maintained for 10 seconds
- Readout with OSL at 100 ˚C with a heating rate of 5 ˚C/s using blue LED at 40 % of the maximum intensity. Resulting in signal S_c (counts)

The parameters in the preheat phase has been adopted from earlier investigations in order to obtain an optimal OSL signal (Zhang et al., 2005) from the salt. The general idea of preheating is to empty unstable, shallow, traps. The parameters for the readout with OSL have also been chosen based on previous investigations of NaCl (Christiansson et al., 2011).

In the present project, the standard readout protocol was shown to change the properties of the NaCl pellets. Because of this, the different parameters of the protocol were investigated to determine which parameter altered the properties of the salt. This lead to the development of a new readout protocol. The new readout protocol that is suggested for the NaCl pellets is composed as follow:

- Unknown dose or given dose, D_u (mGy)
- Readout of OSL at 20 ˚C using blue LEDs at 40 % of the maximum intensity. Resulting in OSL signal S_u (counts)
- Calibration dose, D_c (mGy) using the internal ^{90}Sr/^{90}Y beta source

- Readout of OSL at 20 ˚C using blue LEDs at 40 % of the maximum intensity. Resulting in OSL signal S_c (counts)

The duration of the OSL readout may be adjusted depending on the magnitude of D_u or D_c. Larger absorbed doses might require longer readout times to fully deplete the traps responsible for S_u or S_c.

The signal from the salt S_u or S_c (counts) is determined by integrating the amount of counts registered during the LED-stimulation. The integration interval is defined as the full readout time i.e. OSL stimulation time. By relating the known calibration dose, D_c, to the measured calibration signal, S_c, it is possible to calculate the unknown dose D_u from the value of the OSL signal S_u. If the relationship is linear then $\frac{D_u}{D_c} = \frac{S_u}{S_c}$. An alternative method is to administer several calibration doses of different size to find a linear relationship. This method is called single aliquot regeneration, SAR, and gives, in general, a more accurate result but takes considerably longer time if fully implemented (Christiansson et al., 2011).

The two protocols were compared using the Coefficient of Variation, C_v, which is defined as

$$C_v = 100 \cdot \frac{SD}{\mu} \quad (4)$$

where SD is the standard deviation and μ is the arithmetic mean.

2.4 Irradiation geometries

Co-60 source

Two different ^{60}Co calibration sources were used in the current project, at SUS Malmö and Lund, respectively. The ^{60}Co unit in Malmö is mounted in a 90-degree angle and two fixed distances are used to achieve irradiations at two different dose rates. In the close geometry (51 cm) from the source, the current dose rate is 42.1 mGy/min to water and in the distant geometry (549 cm) the dose rate is 0.40 mGy/min to water. The ^{60}Co unit in Lund is mounted in a 90-degree angle and the current dose rate is 2.96 Gy/min when placing the phantom at a fixed distance on the head insert.

Sr-90/Y-90 source

The Risø TL/OSL reader has an internal ^{90}Sr/^{90}Y calibration source that may be used for verification and calibrations. The OSL-reader is optimized for measurements on quartz and when calibrating the reader to obtain the dose rate, grains of quartz are used. The dose rate to salt is obtained by correcting for the difference in stopping power between quartz and salt. The current dose rate of the internal ^{90}Sr/^{90}Y source is 0.73 mGy/s to salt.

2.5 Optimal Configuration

To determine the optimal configuration of the NaCl pellets, the salt in is its original form as grains, was irradiated in the OSL reader. Each salt (Table 1) was divided into various fractions after grain size distribution. Directly after irradiation the OSL signal, S_u, was acquired and the signal per unit weight was investigated as a function of the different grain sizes. The results were then compared to the amount of each grain size fraction available for the various salts (Fig. 2).

The six different salts were pressed into pellets using different grain sizes and pressures/compression force. Two days after production the weights of the pellets were registered before they were placed in the OSL reader. They were then irradiated by the internal ^{90}Sr/^{90}Y source. The OSL signal was measured using the standard readout protocol. A calibration dose was administered and measured in the same way as the first given dose, the so called unknown dose. To investigate which salt that provided the best response, the signal per unit weight was calculated.

The physical properties of the pellets were also considered as an important factor. Some grain size fractions resulted in pellets that fell apart when handled and some did not form pellets at all. The configurations which did not produce physically stable pellets were directly excluded from further studies.

2.6 Dosimetric properties

The three salts with the best signal per unit weight were pressed into pellets and used in all of the following measurements. To investigate if the signal is influenced by the manufacturing process of the NaCl pellets, the signal stabilization after pellet production was studied. For this purpose, the standard readout protocol in Section 2.3 was used and the OSL-signal per calibration dose was evaluated. This ratio was calculated based on measurements performed 0 h, 6 h. 12 h, 18 h, 24 h, 48 h, 7 days, 14 days and 1 month after the production of the pellets. For each of these readouts, the OSL signal per unit weight was also calculated to investigate the variation with time. When the signal no longer varied significantly between measurements it was considered that the NaCl pellets were stable in regard to the signal per given unit dose.

Many materials become more sensitive to radiation after they have been irradiated. This means that the signal per radiation dose will increase after the material has been exposed to radiation. This is called sensitization and the sensitization of the pellets after repeated usage was investigated by repeated measurements (15 times) using the standard readout protocol in Section 2.3. For every readout, the OSL-signal per calibration dose and the OSL signal per weight was calculated. The sensitization was investigated by comparing the ratios of the OSL signal and the signal from the calibration dose after every repetition of the readout protocol. The OSL signal per unit weight was investigated in the same way.

The dose response was investigated by irradiating NaCl pellets with different absorbed doses, from 3.7 mGy up to about 6 Gy. The near geometry of the ^{60}Co source at SUS Malmö was used as well was the ^{60}Co source at SUS Lund. D_us were chosen so that there was an overlap of two data points; the highest D_u in Malmö and the lowest in Lund. Plotting the signal S_u as a function of D_u reveals the OSL to dose response. This was done for irradiations using the internal ^{90}Sr/^{90}Y source of the OSL reader. When an irradiation source outside of the OSL reader was used, the pellets were irradiated in darkness and then handled under red light. In between irradiation and readout, they were stored in darkness at normal ambient conditions.

Minimum detectable dose, MDD, defined as three times the standard deviation (Currie, 1968) of the natural background signal multiplied with the specific luminescence (Bernhardsson et al., 2009), was determined by performing an OSL-readout on 10 identical (made from the same brand of salt using the same compression force and grain size fraction) NaCl pellets which had not been previously irradiated. The resulting background signals were integrated over the readout time and the standard deviation was calculated. The MDD was then calculated by the use of the specific luminescence of the salt. The specific luminescence was

calculated as the average signal per administered dose with data from dose response measurements. The MMD, minimum measurable dose, defined as 10 times the standard deviation (Currie, 1999) of the background signal multiplied by the specific luminescence was also calculated.

After exposure to ionizing radiation the stored signal in any material used for dosimetry might change. When the signal decreases with time it is called fading and if the signal increases with time, it is called inverse fading (Christiansson et al., 2014). To investigate the fading of the signal in salt, pellets were irradiated with 108 mGy in a ^{60}Co beam. The signal from the pellets was then measured 0 h, 6 h. 12 h, 18 h, 24 h, 48 h, 72 h, 7 days, 14 days, 1 month and 2 months after irradiation, after being stored in darkness at normal ambient conditions in the laboratory.

The short time initial fading after irradiation was investigated separately by performing readouts of the OSL signal at various short times after irradiation in the OSL reader. Short pauses on the scale of seconds were introduced before readout.

2.7 The dosimeter

In order for a material to work as a dosimeter the energy response must be similar to that of human tissue. For salt this is true for photon energies above about 200 keV, but for lower energies there is an over response in the salt due to the higher effective atomic number of salt (Z_{eff} = 14.0) compared to tissue (Z_{eff} = 7.35). A simplified energy response of salt versus tissue was calculated using data from NIST's databases (Hubbell, J.H. and Seltzer, 2004). By the use of filters of different materials and thicknesses, the energy response ratio was altered. The goal was to find a filter which, together with the salt, gives the same energy response as tissue also for low photon energies.

3 Results and discussion

3.1 Optimal pellet configuration

Figure 6 shows the OSL signal per unit weight for the six different kinds of salts investigated, when measured in their original form as grains. In Fig. 7 the same results as in Fig. 6 are shown, but Falksalt 1 and measurements on grains smaller than 100 µm have been excluded for a better overview and comparison.

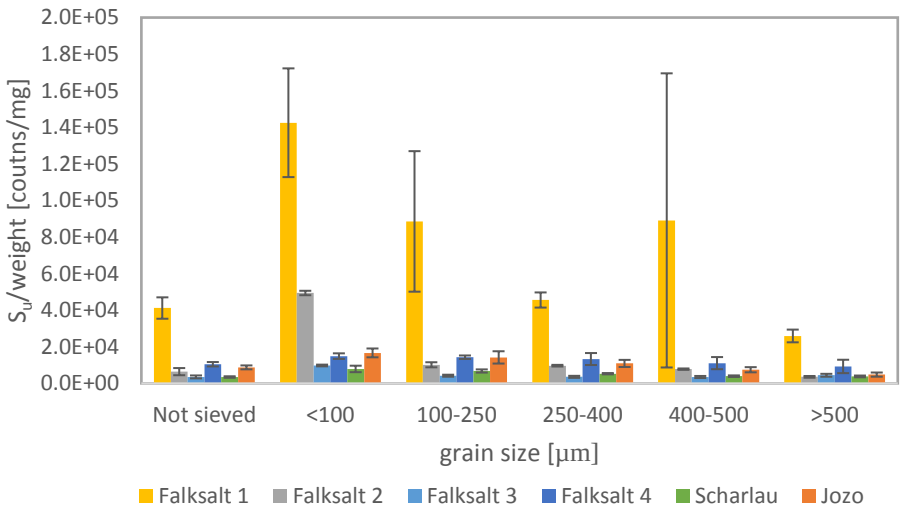

Figure 6. OSL signal S_u per unit weight for the six different salts divided by grain size fractions, after exposure to 7.3 mGy (^{90}Sr). The bars in the graph is the average result from 5 cups of salt, where the uncertainty bars represent ±1 SD of S_u/weight

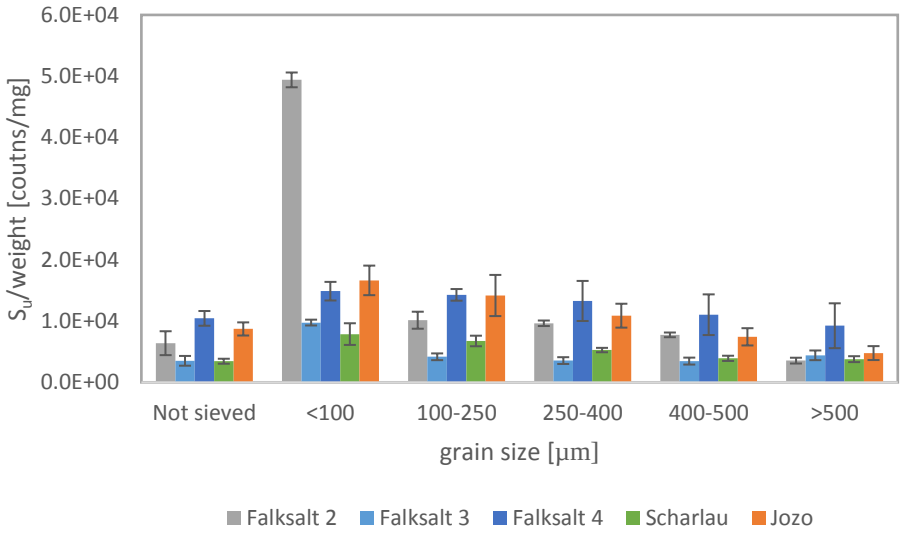

Figure 7. OSL signal S_u per unit weight for five of the salts investigated. Falksalt 1 and the measurements on grains smaller than 100 µm have been excluded as compared to Figure 6. Every bar in the graph is the average result from 5 cups of salt, where the uncertainty bars represent ±1 SD of S_u/weight.

When measurements where done using grains of salt, the signal per unit weight was highest in the Falksalt 1 and generally for grains below 100 µm (Fig. 6). However, the OSL curve of Falksalt 1 differ significantly compared to the OSL curves of the other salts. In the OSL curve of this particular salt, the signal does not become zero, i.e. the stored signal is not depleted but stays at an unknown level even after extended light stimulation. The signal never reaches a low background and because of this the signal appears to be larger than it actually is. Further, since less than 1% of the salt in the containers (of all brands) are of sizes smaller than 100 µm this size was excluded in the further investigations. Even more important, grains of this size are not suitable for pressing to pellets as they tend to form physically unstable units.

Using various compression force (1.5-3.0 T) pellets were made from the six different salts investigated. The results from measurements on these NaCl pellets are presented in Figure 8.

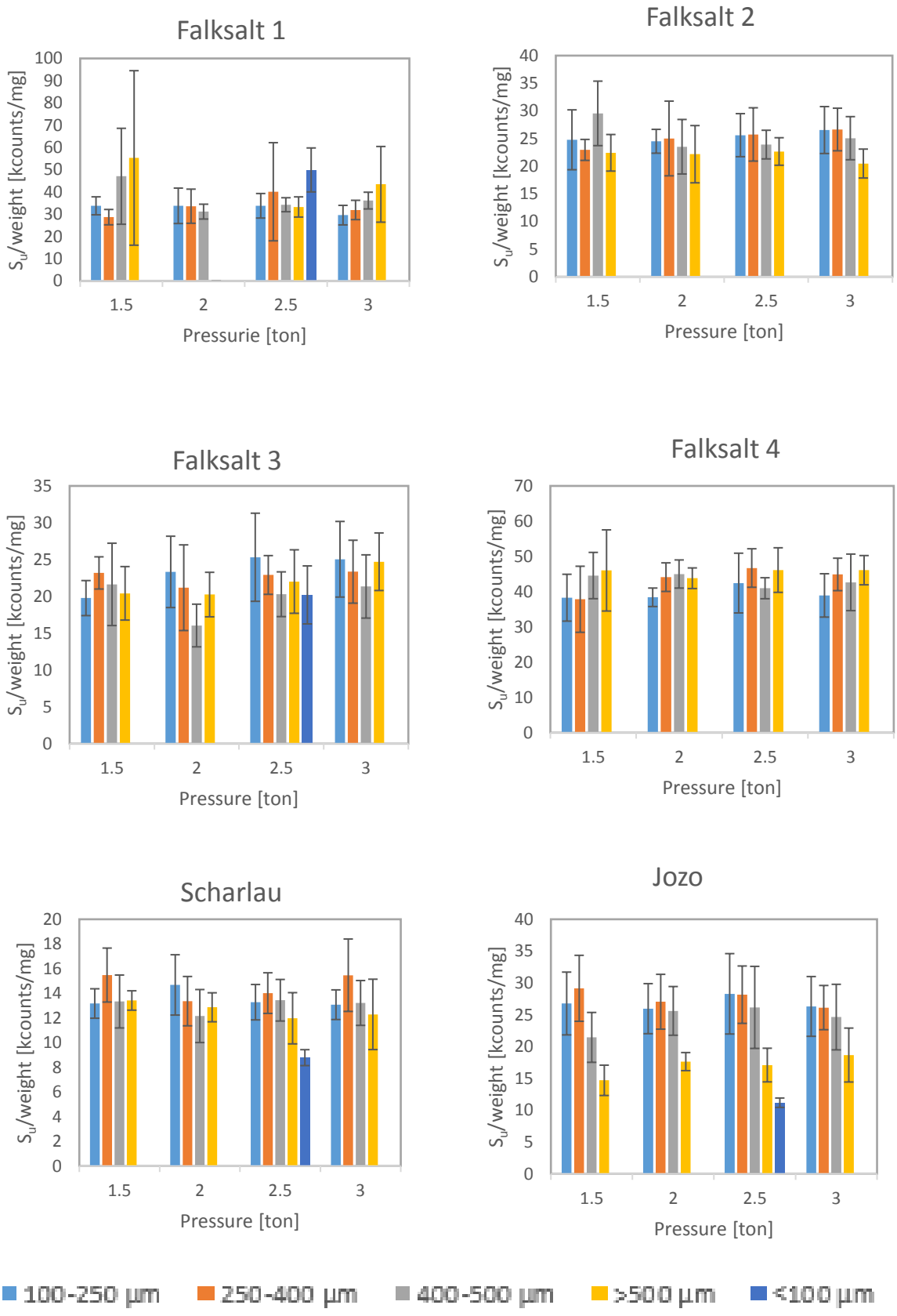

Figure 8. Graphs A-F shows the signal, S_u, per unit weight for different pellet configurations in terms of salt grain size fractions and compression force. The bars in the graphs correspond to the average measurements of five NaCl pellets made from different grain sizes as indicated by the key. For every salt and for the different grain sizes, pellets were pressed with 1.5, 2.0, 2.5 and 3.0 tons of compression force. The uncertainty bars representing ±1 SD of S_u/weight.

Based on the results from both grain and pellet measurements, 3 salts were chosen for further investigations. Since it was a very little amount of material to make pellets from for salt grains <100 µm and because they easily fell apart, this fraction was excluded.

Using a higher compression force doses not change the signal from the pellets much but they became harder and did not fall apart as easily. When making the pellets it was also found that the size fractions 100-250 µm and 250-400 µm achieved the physically most stable pellets.

As suspected from the measurements on the salt in its grain form, Falksalt 1 have the highest signal per unit mass, but this is because the glow curve never reaches a stable low background (See Appendix B). When integrating over the readout time this will lead to a misleading, higher signal. Because of this, Falksalt 1 was excluded as a potential salt for producing NaCl pellets for dosimetry. In Falksalt 4 however, the signal per unit weight is higher than for the other salts but this salt contains rather little of the preferred size fractions according to Fig. 3. Hence, at this stage of the study Falksalt 4 was excluded. Falksalt 2 and 3 give similar signals per unit weight whereas with Falksalt 3 it was achieved better pellets in terms of the mechanical properties. These observations and the fact that there are a lot of previous measurements on Falksalt 3, it was decided to exclude Falksalt 2. The Scharlau salt gave the lowest signal per unit weight but was kept in the further investigations as it is chemically pure and a commonly available reference. The fact that it contains less impurities than commercially available salt like Falksalt and Jozo may explain why the signal is lower for the Scharlau salt. In addition, Jozo gave a higher signal than Falksalt 3 and was also included in the further investigations.

Falksalt 3, Scharlau and Jozo have been used in all the following investigation. For Falksalt 3, grain sizes of 100-250 µm was used and for Scharlau and Jozo, grain sizes of 250-400 µm were used. All pellets were pressed with a compression force of 3.0±0.5 tons.

3.2 Dosimetric properties of salt

Signal stabilization after pellet production

The results of measurements, using the standard protocol from Section 2.3, on the NaCl pellets at different times after production are presented in Figure 9. In the left graph D_u was 36.5 mGy and D_c 7.3 mGy, corresponding to a theoretical ratio of 5. In the right graph, the new readout protocol was used, and both D_u and D_c were 7.3 mGy, corresponding to a theoretical ratio of 1.

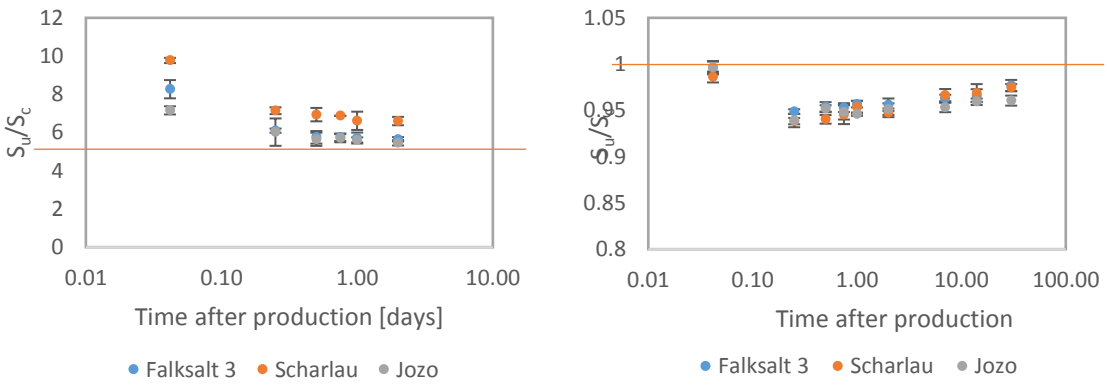

Figure 9. The signal ratio S_u/S_c at different times after pellet prduction. In the left graph D_u was 36.5 mGy and D_c 7.3 mGy. The theoretical ratio of 5 is indicated by a red line. The standard readout protocol in section 2.3 was used. In the right graph

both D_u and D_c were 7.3 mGy, with a theoretical ratio of 1, that is indicated by a red line. The new readout protocol was used. Every data point in the graphs is the average result from five NaCl pellets and the uncertainty bars representing ±1 SD of S_u/S_c.

In the left graph in Figure 9 the ratios are higher than the theoretical value after all time delays between production and usage. When this was noticed the readout protocol was investigated, as shown below. After an adjustment of the readout protocol (no preheat and OSL signal readout at room temperature) the measurements were repeated and the results are presented in the right graph in Figure 9. Here the signal ratio S_u/S_c is within 6% at all the studied time delays. Figure 9 also shows that the signal starts to stabilize after about 6 hours after production of the NaCl pellets, even though the ratio does not reach the theoretical value. The point in time after the NaCl pellet production when the pellets are ready to use and a high reproducibility is expected, is further illustrated in Figure 10.

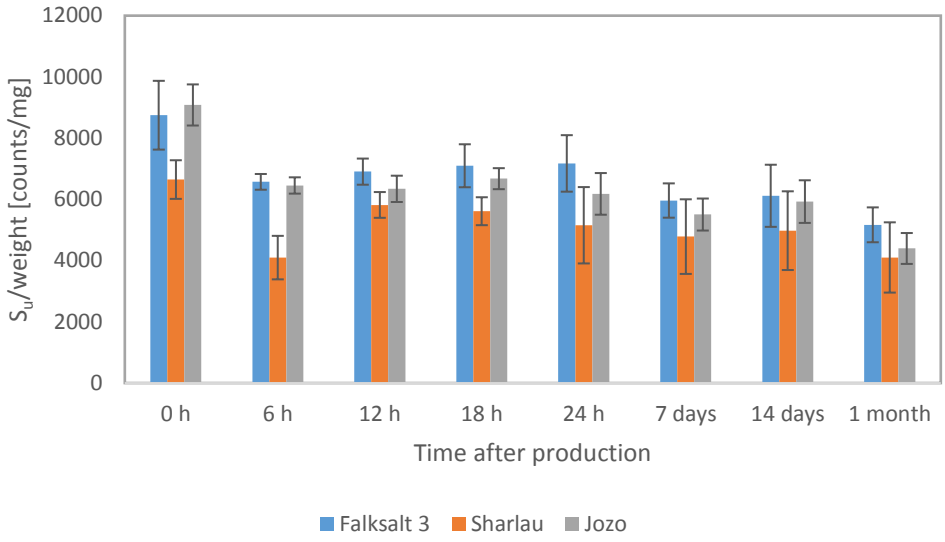

Figure 10. S_u per unit weight at different times after pellet production. Every bar in the graphs is the average result from five NaCl pellets, with uncertainty bars representing ± 1 SD of S_u/weight.

Sensitization with standard protocol

The sensitization was investigated using the standard protocol in Section 2.3. The protocol was repeated 15 times on the same NaCl pellets and the result is presented in Figure 11. Each data point corresponds to the average S_u/S_c of five NaCl pellets. The given D_u and D_c were both 7.3 mGy.

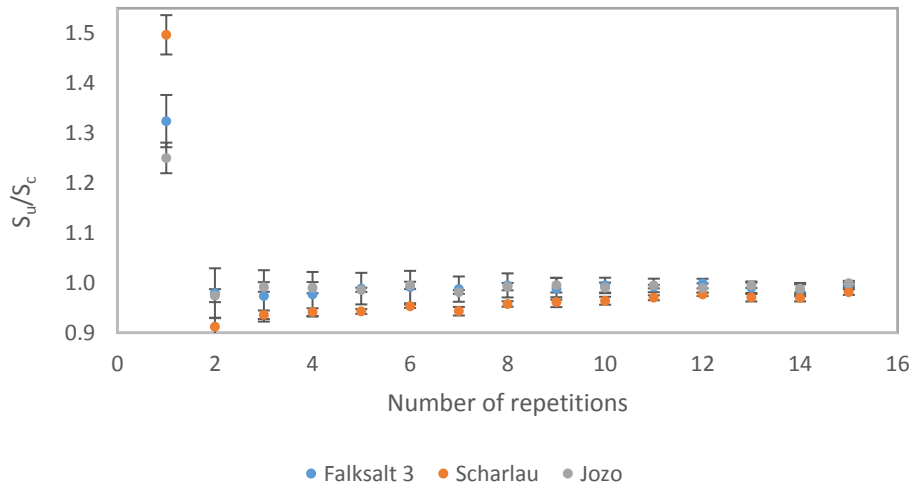

Figure 11. The result of repeating the standard readout protocol 15 times on the same pellets. The resulting data points correspond to the average of 5 pellets. The given D_u and D_c where7.3 mGy, meaning a theoretical ratio of 1. The uncertainty bars representing ±1 SD of S_u/S_c

The first readout of the pellets show a ratio which is higher than expected but the following repetitions show a ratio close to one. This means that the properties of the salt change during the first readout. Since the ratios are similar after the second repetition, the properties of the salt are not altered between readout two and 15. The results presented in Figure 11 led to the development of a new readout protocol.

Development of new readout protocol

In the left frame of Figures 9 and 11 the signal ratio S_u/S_c is too high for the calibration dose to directly estimate the unknown dose correctly. Since the ratio is larger than the theoretical value, the signal from the calibration dose is smaller than it should be. Because of this, the standard readout protocol was investigated. At least one of the processes in the standard protocol alters the properties of the salt prior to the second irradiation.

To determine which process is responsible for the change in the S_u/S_c ratio, a sequence was run in which the different steps in the standard readout protocol that precedes the second irradiation was performed. After this the standard protocol was performed on the same pellets. The results are presented in Figure 13. Since the parameter which affects the ratio will already have altered the properties of the salt when the standard protocol is performed, the ratio should be close to 1.

Figure 12. The three different steps in the standard readout protocol which precedes the second round of irradiation. Data at point 1 corresponds to 10 seconds of irradiation before the standard protocol, data at point 2 corresponds to a preheat at 220° C for 10 seconds before the standard protocol and data at point 3 corresponds to an OSL readout for 10 seconds before the standard protocol. The given D_u and D_c where7.3 mGy, meaning a theoretical ratio of 1. Every data point in the graph is the average result from five NaCl pellets, with uncertainty bars representing ±1 SD of S_u/S_c.

The results in Figure 13 conclude that the heating of the NaCl pellet before irradiation changes the sensitivity. When the salt is heated, it becomes less sensitive and therefore the S_u/S_c ratio is higher than is should be. When the first dose is administered to the NaCl pellet the salt has not been heated but the preheat before the readout changes the sensitivity before the calibration dose is administered. Based on the result in Figure 13 the preconditions of the pellets were altered. To avoid the heating effect in the middle of the protocol, the pellets either need to be heated before the first irradiation or not heated at all before the second irradiation.

In Figure 14 the results of changing the preconditions of the pellets are presented. In three cases (altered readout parameters 1-3 in Fig. 13) the preheat in the standard protocol was eliminated and the readout temperature was varied. In three other cases (altered readout parameters 4-7 in Fig. 13) the pellets were preheated in the OSL-reader and in an oven before the standard protocol from Section 2.3 was performed.

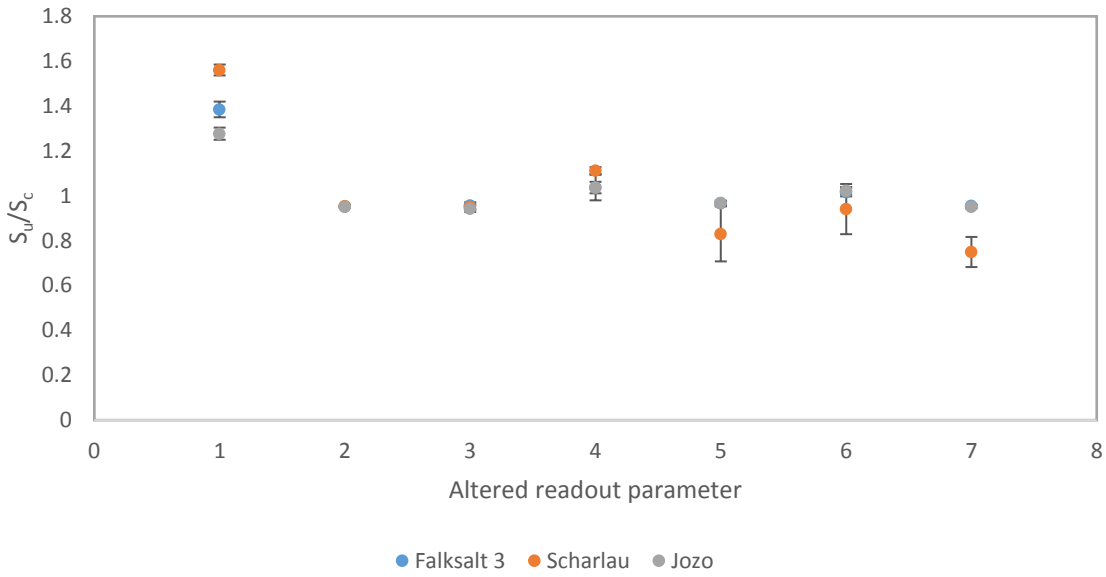

Figure 13. Influence of various precondictions on the NaCl pellets when readout by the standard protocol. At datapoint 1 the results of the standard protocol are presented, at datapoint 2 the preheat was excluded and the OSL was performed at room tempereature, at datapoint 3 the preheat was excluded and OSL perdormed at 100°C, at datapoint 4 the preheat was excluded and OSL performed at 150°C, at datapoint 5 the pellets were heated for 10 seconds at 220°C in the readout unit before readout, at datapoint 6 the pellets were heated in an oven at 220°C for 5 minutes before readout and at datapoint 7 the pellets were preheated at 220°C for 10 minutes in an oven before readout. The datapoints are the resulting averages of 5 pellets. The given D_u and D_c where 7.3 mGy meaning a theoretical ratio of 1., with unceratinty bars representing ±1 SD of S_u/S_c.

In Figure 14 datapoints 5, 6 and 7 show that heating the pellets outside of the OSL reader before measurements introduces uncertainties for Scharlau. Eliminating the preheat (datapoints 2, 3 and 4 in Fig. 14) yield ratios around 1. Since the uncertainties were smallest when readout was performed without preheat and at room temperature, this was introduced in the new readout protocol presented in Section 2.3.

Sensitization with new readout protocol

In Figure 12 are the result of not pre-heating the pellets and performing the readout at room temperature (new readout protocol in Section 2.3). The given D_u and D_c were both 7.3 mGy. The sequence was repeated 15 times.

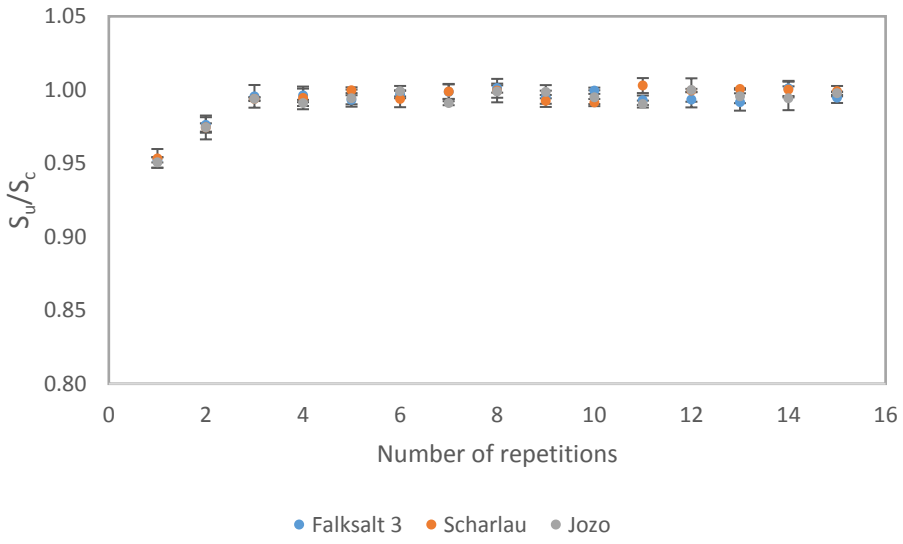

Figure 14. Sensitization of the pellets when the new readout protocol was used. The sequence was performed 15 times on each pellet. The resulting data points are the averages of 3 pellets. The given D_u and D_c where 7.3 mGy, meaning a theoretical ratio of 1. The uncertainty bars representing ±1 SD of S_u/S_c.

According to Fig. 12, not heating the NaCl pellets results in a maximal error of 5% the first time the pellets are used. The average coefficient of variation, C_v, for all repetitions was calculated to investigate if the new protocol affects the standard deviations. Calculations show that the average C_v is reduced from 0.9% to 0.4 % for Falksalt 3, from 2.7% to 0.4% for the Scharlau salt and from 1.0% to 0.4% for the Jozo salt. This means that the variation in readouts is smaller when using the new readout protocol, even though fewer NaCl pellets were used. From repetitions 3 to 15 the error is only about 1%. However, there is a slight change in sensitivity between repetitions 1 and 3 which could indicate that also the new protocol is altering the properties of the salt between readout repetitions, at least initially and to a smaller extent.

Dose Response

The dose response measured per unit weight is presented in Figure 15. The new readout protocol in Section 2.3 was used with a fixed D_c of 7.3 mGy. The salt was irradiated using the internal $^{90}Sr/^{90}Y$ source of the OSL reader.

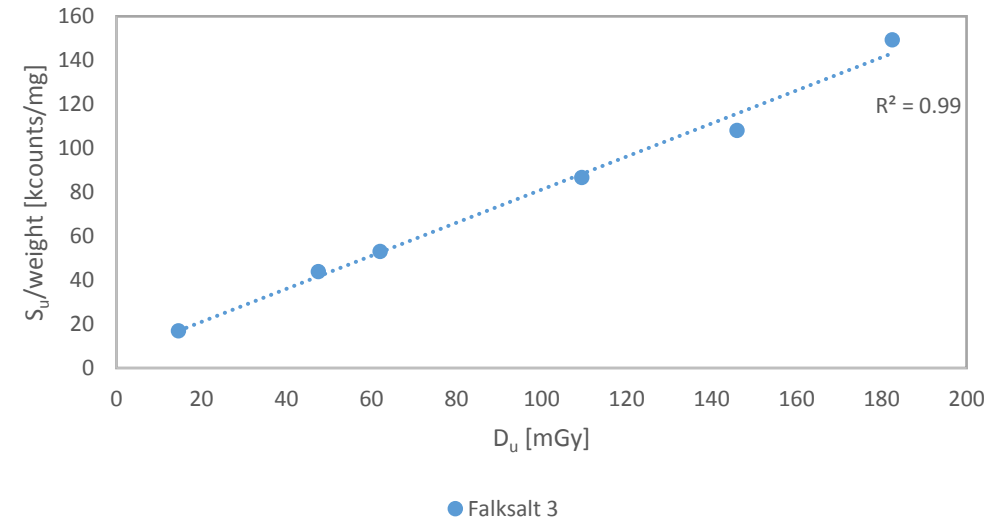

Figure 15. Dose response using the new readout protocol and a fixed D_c of 7.3 mGy. Every data point in the graph is the average result from three NaCl pellets.

When normalized to the weight, the signal is linear up to at least 150 mGy according to Figure 15. In Figure 16 the dose response is presented as the estimated doses as a function of the theoretical given doses.

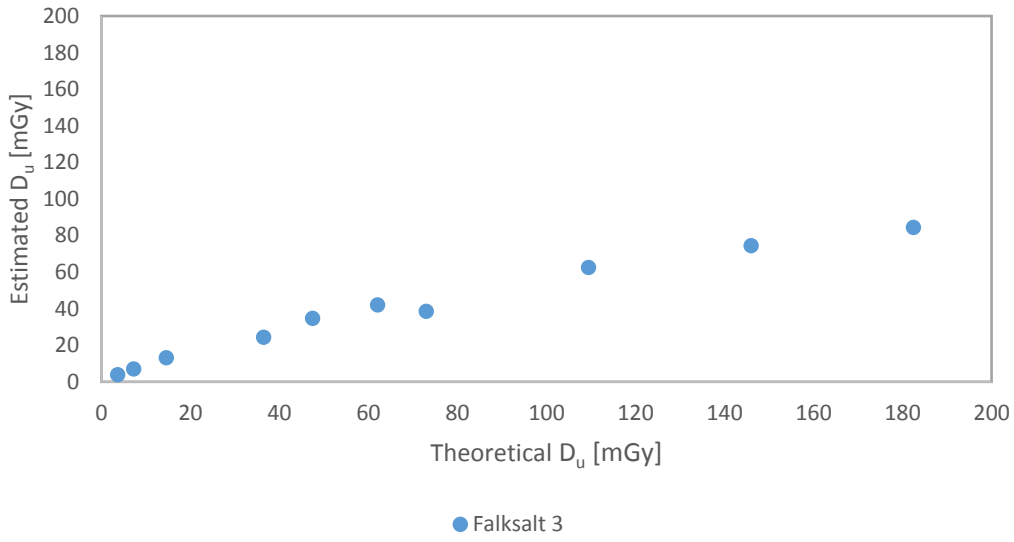

Figure 16. The S_u/S_c ratio using a fixed D_c of 7.3 mGy. Every data point in the graph is the average result from three NaCl pellets.

Figure 16 shows that one small calibration dose is not sufficient to estimate doses correctly. As an outcome of this result, measurements were performed with D_c´s both smaller and larger than D_u to investigate D_c's effect on the signal ratio. The result is presented in Figure 17.

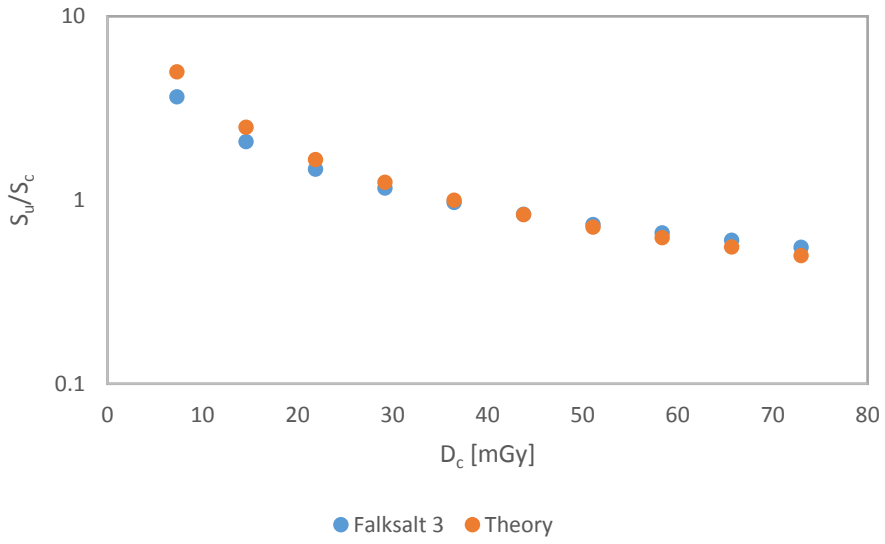

Figure 17. The signal ratio S_u/S_C for a fixed D_u of 36.5 mGy with D_c between 3.6 mGy and 73.0 mGy. Every data point in the graph is the average result from three NaCl pellets.

The deviation from the theoretical value in Figure 18 is shown in Figure 19.

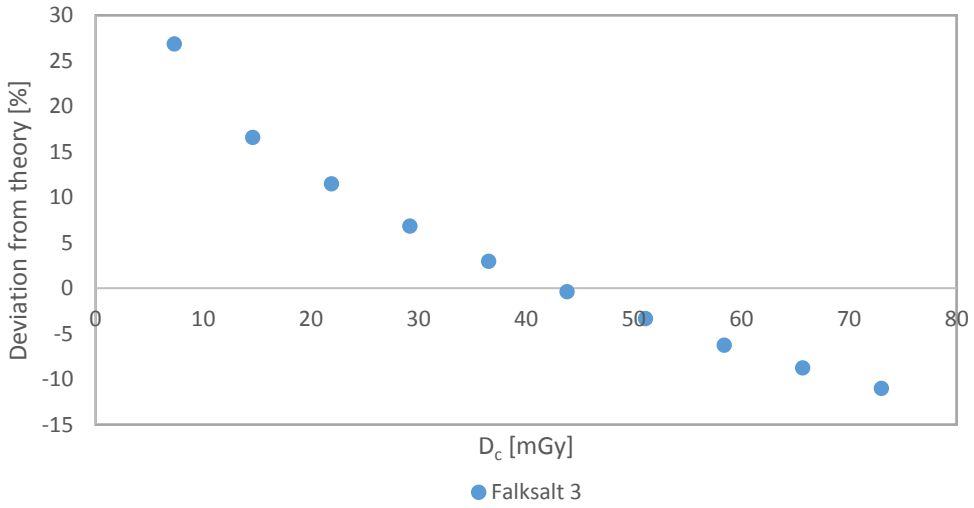

Figure 18. The difference, measured in percent, between the measured and theoretical ratio presented in figure 18. Every data point in the graph is the average result from three NaCl pellets.

From Figures 17 and 18 it can be concluded that a calibration dose that is either too small or too large, as compared to the unknown dose, will introduce errors in the dose estimations. From this result, it is suggested that the calibration dose should be in the same size as the unknown dose in the subsequent measurements.

In Figure 19 the dose responses for the three different salts, when irradiated in the $^{90}Sr/^{90}Y$ of the OSL reader, are presented. D_u was varied between 4 and 1460 mGy, and D_c was the same as D_u.

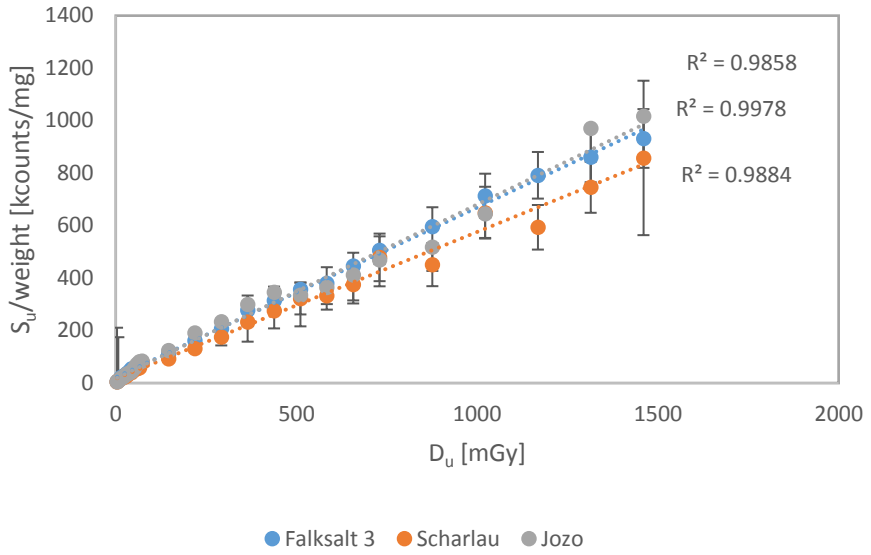

Figure 19. Dose response for three different salts in terms of weight normalized OSL signals of the NaCl pellets. Every data point up to 73 mGy in the graph is the average result from three NaCl pellets and for larger doses it is the average result from five pellets. The unceratinty bars represent ±1 SD of S_u/weight.

From Fig. 19 it is possible to identify that the dose response is linear up to at least 1500 mGy. Presented in Figure 20 are the result of using the same D_u as D_c for the dose estimations.

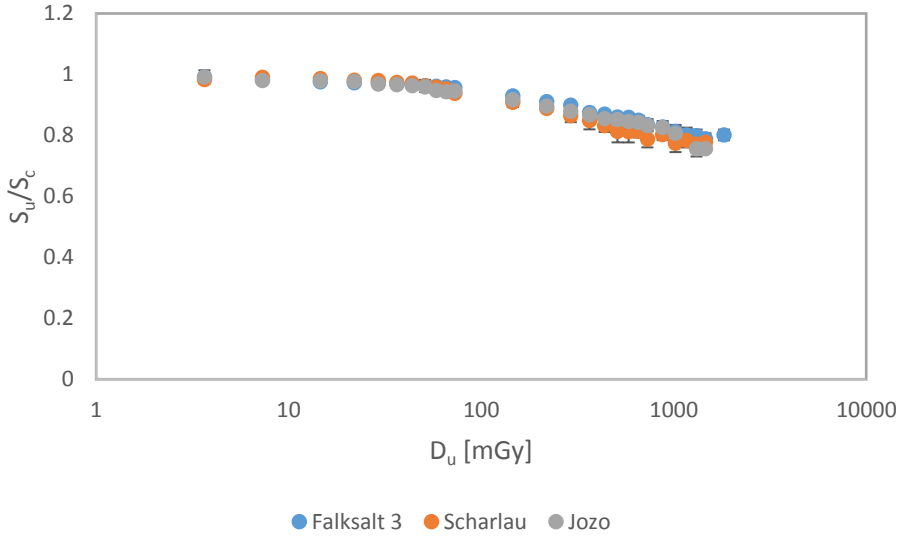

Figure 20. The same dose response data as presented in figure 20 but normalized to the calibration signal S_c. Every data point up to 73 mGy in the graph is the average result from three NaCl pellets and for larger doses it is the average result from five pellets. The uncertainty bars represent ±1 SD of S_u/S_c.

Up to about 100 mGy the signal ratios S_u/S_c are within 6% of the theoretical value. Above 100 mGy however, the ratio gets smaller which means that the estimated dose will be lower than the theoretical (true) value. Since the ratio is smaller than the value 1 this means that the calibration dose is too large. An explanation for this is the sensitization of the salt. When the salt is exposed to radiation during the first given dose it becomes more sensitive and when the

calibration dose then is administered the signal per unit weight is higher. This and that the effect is increasing with the initial given dose can also be seen in Figure 21.

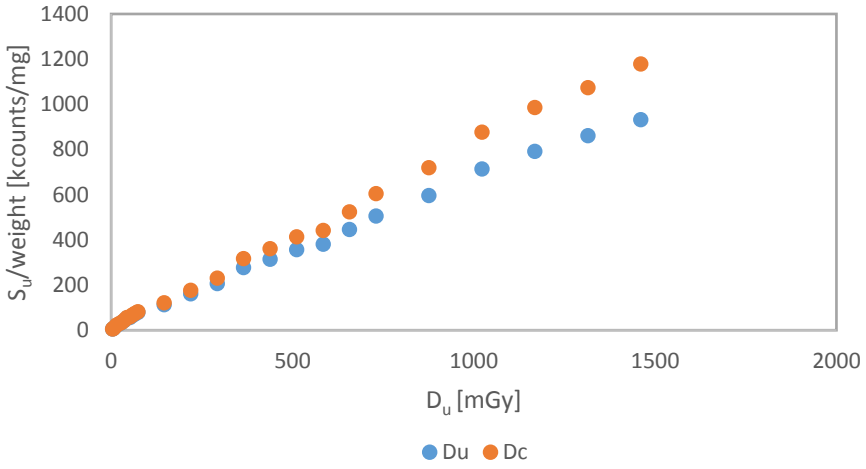

Figure 21. The graph shows the change in sensitivity between D_u and D_c as the dose D_u increases. Every data point up to 73 mGy in the graph is the average result from three NaCl pellets and for larger doses it is the average result from five pellets.

From Figure 21 it is clear that there is a change in sensitivity between the first and second irradiation and that the size of the first irradiation affects the size of this sensitivity change.

To make sure that the new readout protocol is not the reason for the errors in dose estimations (Figs. 16 and 20) a dose response was measured with the standard protocol. D_c was 7.3 mGy and D_u was varied between 73 and 365 mGy. Another measurement was done when D_C was chosen to be the same as D_u. The result of using the standard protocol with a small calibration dose is shown in the left frame of Figure 22 and the result of using calibration doses of the same size as the unknown doses is shown in the right frame of Figure 22.

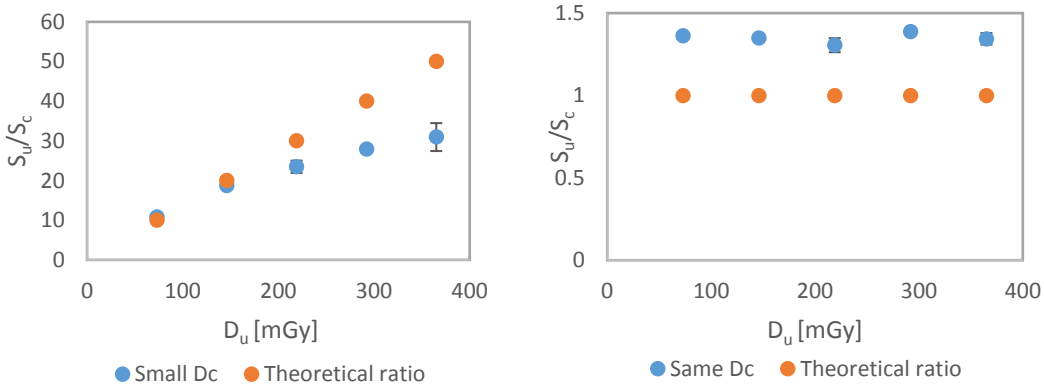

Figure 22. Dose response measurements using the standard protocol. In the left frame, a small D_C of 7.3 mGy was used and in the right frame D_C was the same as D_u. The uncertainty bars represent ±1 SD of S_u/S_c.

The dose response of the NaCl pellets was also investigated using a ^{60}Co beam. Figure 23 shows the resulting signal as a function of administered dose.

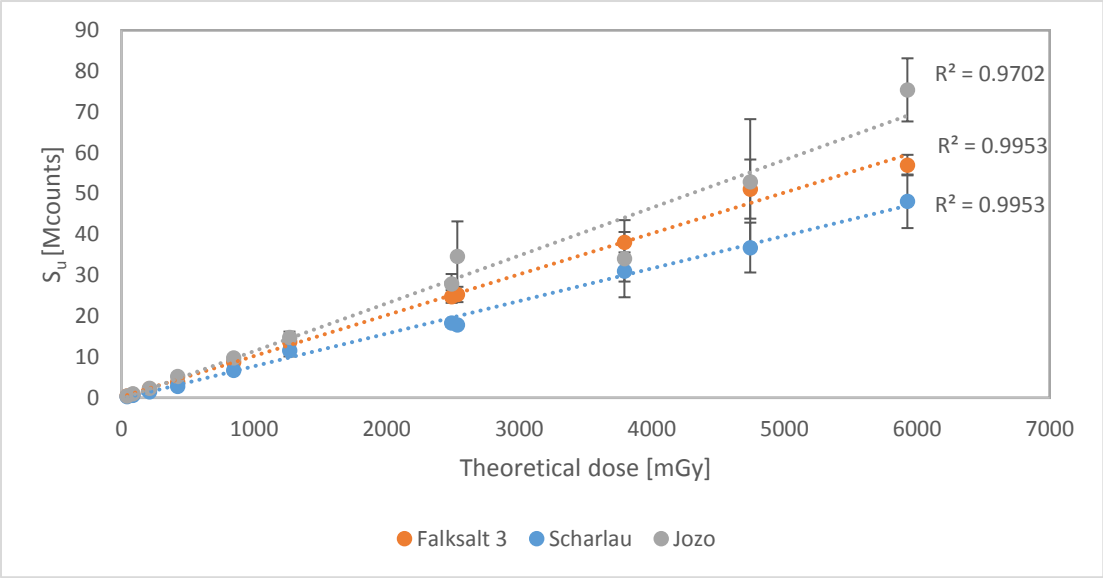

Figure 23. The dose (mGy) response (10^6 ×counts) of NaCl pellets in a ^{60}Co beam. Doses below 2 Gy were administered at SUS Malmö and doses larger than 2 Gy were administered at SUS Lund. Every data point in the graph is the average result from 5 pellets. The uncertainty bars represent ±1 SD of S_u.

The signal was not weight normalized in the results presented in Figure 23 but the signal is still linear up to about 6 Gy. This is encouraging as it means that the NaCl pellets are homogenous in terms of the size and dosimetric properties. The doses larger than about 2 Gy show larger uncertainties than lower doses, probably because of the limitations of the PMT to measure high signals (several Mcounts).

Estimations of the administered doses based on the signals in Figure 23 and a small calibration dose is shown in Figure 24.

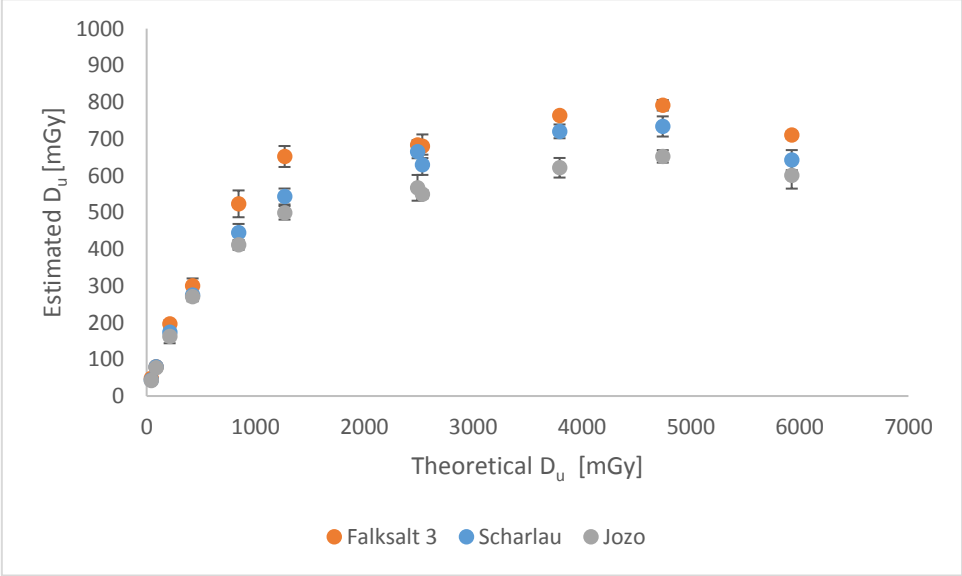

Figure 24. Dose respons in a ^{60}Co beam. The signal is normalized to the calibration signal, D_c. The unknown doses D_u was varied between 42 mGy and 6 Gy, and D_c was 73 mGy. Every data point in the graph is the average result from 5 pellets. The uncertatinty bars represent ±1 SD of the estimated D_u.

It can be concluded from Fig. 24 that a calibration dose of 73 mGy is not enough to correctly estimate high unknown doses and that another readout protocol is needed to estimate high doses, >100 mGy.

3.5 Short term fading

In Figure 25 the weight normalized signals from the dose response investigations (Fig. 19) have been divided by the irradiation time to show the impact of different irradiation times on the signal from the salt.

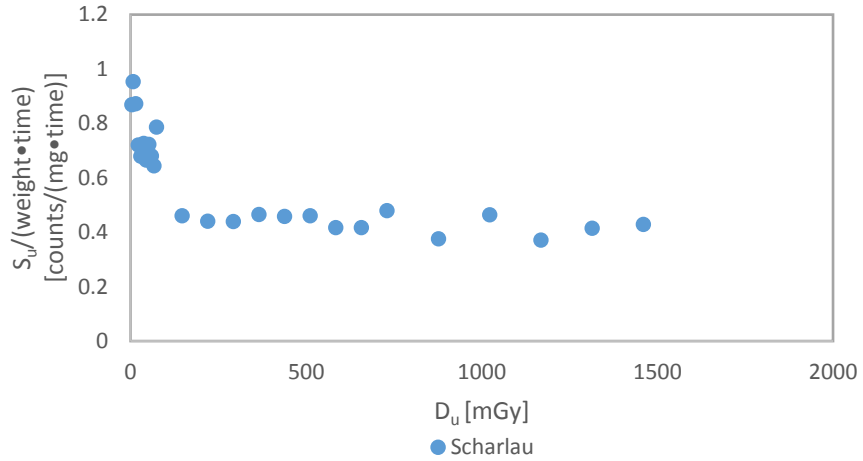

Figure 25. The signal per unit time. The signals from the dose response was normalized to the weight and irradiation time. Every data point up to 73 mGy in the graph is the average result from three NaCl pellets and for larger doses it is the average result from five pellets.

For shorter irradiation times the signal per unit time is higher than for longer irradiation times. Since the dose rate from the $^{90}Sr/^{90}Y$ solely depends on natural decay this must be constant and therefor the dose rate effect must come from the salt. To investigate this further NaCl pellets were irradiated and readout at intervals, from 0-1700 seconds. The results of this investigation, with a D_u of 7.3 mGy, are presented in Figure 26.

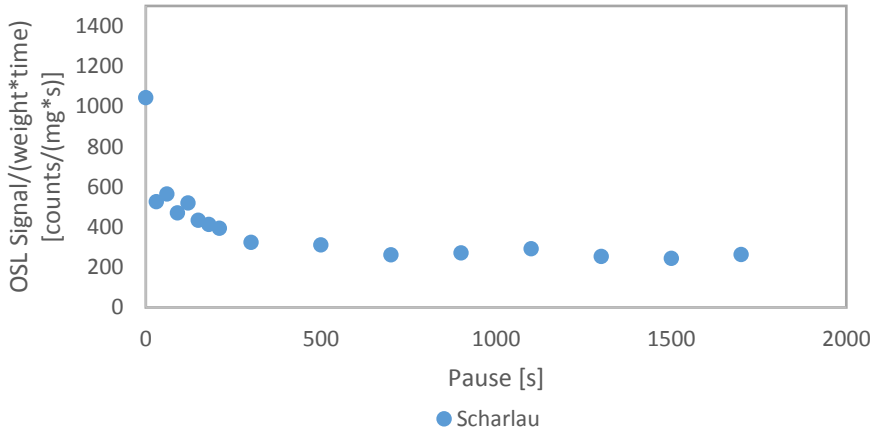

Figure 26. Weight normalized OSL signals when performing readout of the OSL signal at different times after irradiation. Pauses between 0 and 1700 seconds were introduced between irradiation and readout.

The doses in Figure 25 are higher than those in Figure 26 but the graphs show similar trends. Figure 26 shows that readouts right after irradiations give higher signals than if a pause is introduced before readout. This means that some of the signal is lost between irradiation and readout, probably because of some stabilization of the traps. For the longer irradiation times

in Figure 25 the loss of signal and stabilization of traps occurs during the irradiation which is why the signal per unit time is smaller.

This phenomenon is important because it affects the dose estimations. If the salt is used as a dosimeter and it accumulates dose for a longer period, the traps will have time to stabilize and this short time fading of the signal will not be a problem. The problem occurs when the calibration dose is administered and readout close in time to each other. If the calibration dose is read out straight away the signal will be higher and the estimated dose will be lower than if the calibration signal was read out after it had time to stabilize.

Figure 27 shows a dose response curve of NaCl pellets (Scharlau) measured with the new readout protocol but with a pause of 200 seconds before the signal readout. The 200 second pause was chosen based on the results of Figure 26, where the signal starts to stabilize after about 200 seconds.

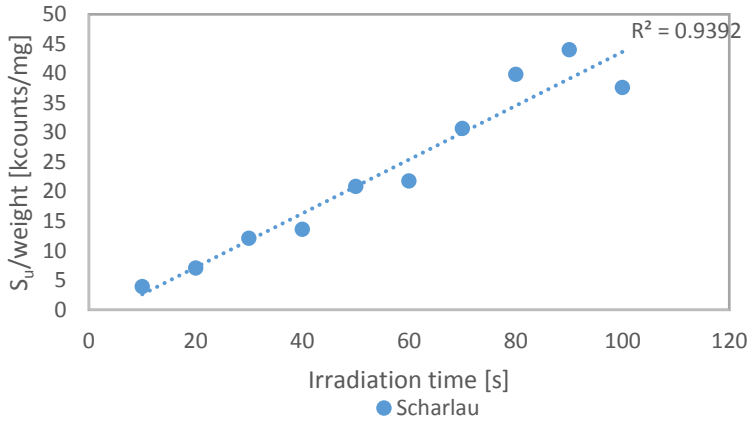

Figure 27. Dose response (in terms of irradiation time (s) in the $^{90}Sr/^{90}Y$ source) as measured with the new readout protocol but with a 200 second pause introduced before readout. Every data point represents the result of one pellet.

The dose response is linear also when a pause is introduced before the readout. Only one pellet was used per data point which could explain why the dose response is slightly less linear than in for example Figures 19 or 23 that are averages of three or five NaCl pellets.

Figure 28 presents the signal per unit time when pauses have been introduced before readout. The dose response has been divided by the irradiation time.

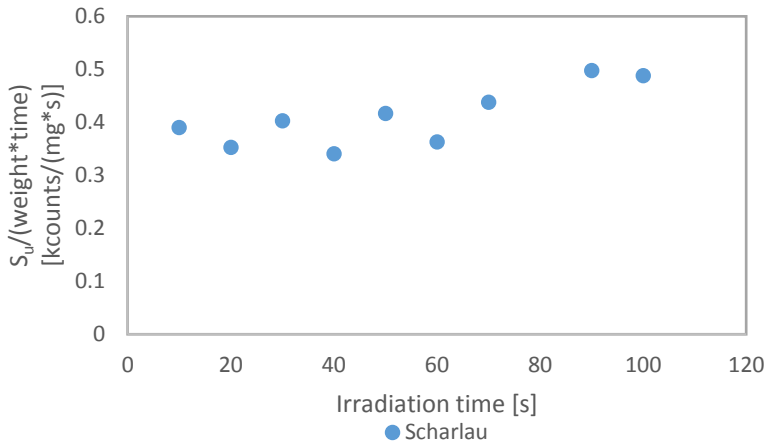

Figure 28. The weight normalized signal per unit time for the same dose response data as in Figure 27.

Comparing Figures 25 and 28, the signal is more stable in Figure 28 where a pause has been introduced before signal readout. The slight increase in signal with longer irradiations could be explained by the fact that the pause was introduced after all the irradiation, which means that there is a time difference between readouts. It could also be an effect of the increasing dose and that for higher doses it takes longer time for the signal to stabilize.

Long term fading

Investigations of the long time fading of the OSL signal are presented in Figure 29. D_u was 108 mGy and D_c was 7.3 mGy. In Figure 11 the left frame corresponds to readouts using the standard protocol in Section 2.3 and the right frame correspond to readouts with the new readout protocol. The signals at different times, $S_{u,n}$, have all been normalized to the first value $S_{u,1}$, to see how the signal varies over time.

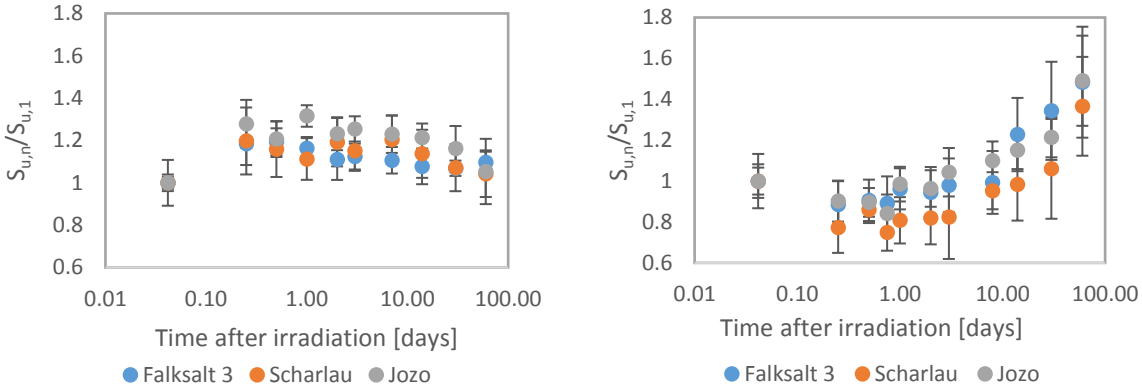

Figure 29. Signal measurements performed on pellets at various times after irradiation. The signal values $S_{u,n}$ have all been normalized to the first value $S_{u,1}$, readout 1 h after irradiation. The results in the left graph were obtained using the standard readout protocol and the results in the right graph were obtained using the new readout protocol. Every data point in the graphs is the average result from five NaCl pellets. The uncertainty bars represent ±1 SD of S_u/S_c.

The graph in the left frame of Figure 29 shows the fading measured with the standard readout protocol, where an initial inverse fading is indicated during the first hours. This is followed by a small fading of the signal after about 10 days. In the right frame of Figure 29, the signal fading is the opposite: during the first hours, there is a small fading and after about 7 days there is an inverse fading of the signal. One explanation to this signal increase may be electron tunneling, electrons at traps which cannot be emptied with the blue LED tunnel to

traps which can be emptied. It cannot however be explained by accumulation of background radiation during storage.

3.5 Minimum detectable dose

The minimum detectable dose and minimum measurable dose for the NaCl pellets, calculated as described in Section 2.6, is presented in Table 2 together with the specific luminescence for the three salts.

Table 2. The minimum detectable dose, minimum measurable dose and specific luminescence for the three salts.

Salt	**3*SD of background signal [counts]**	**MDD [µGy]**	**MMD [µGy]**	**Specific luminescence [counts/(mg·mGy)]**
Falksalt 3	107	3.7	12	920
Scharlau	155	5.5	19	790
Jozo	98	6.3	21	925
Empty Cups	257	N/A	N/A	N/A

According to Table 2 the MDD is around 5 µGy for the different salts which is very low. This can be compared with e.g. TLDs of LiF:Mg, Ti (TLD-100) that has a detection limit of 10 µGy (Kortov, 2007). The specific luminescence is higher for the salt bought in the store than for the chemically pure salt, probably because they contain more impurities.

3.2 Dosimeter

Because of the energy dependence of the salt, filters are needed for the NaCl pellets to function as a dosimeter. In Figure 30, the theoretical energy dependence ratio of salt and tissue is presented. The ratio is calculated by the use of the mass attenuation coefficients of salt and tissue, taken from the NIST database X-Ray Mass Attenuation Coefficients (Hubbell, J.H. and Seltzer, 2004). These calculations do not take scattered radiation into account which might further influence the shape of the curve.

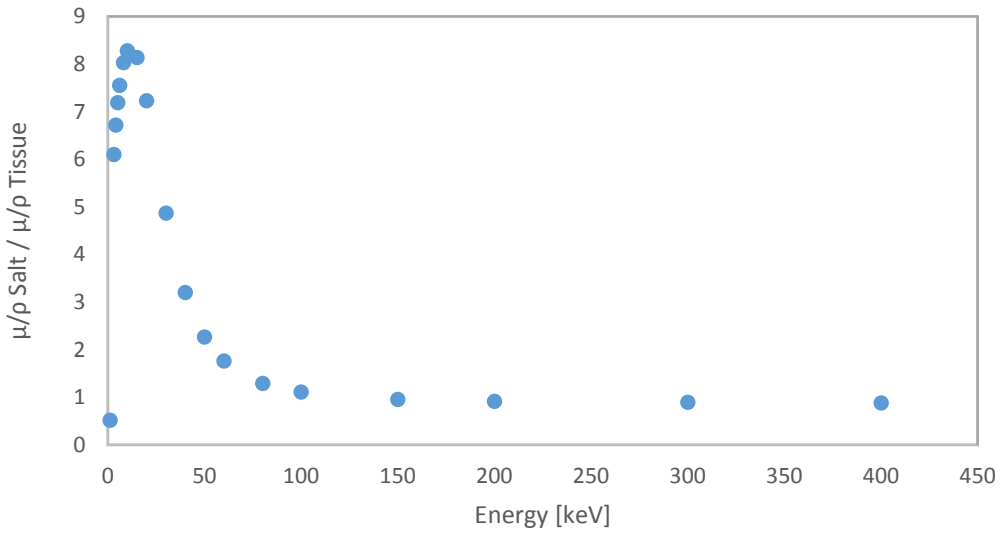

Figure 30. Theoretical energy response ratio for salt and tissue, based on data from the NIST database X-Ray Mass Attenuation Coefficients.

In Figure 31 the result of applying a filter to the salt is presented for three different filter combinations.

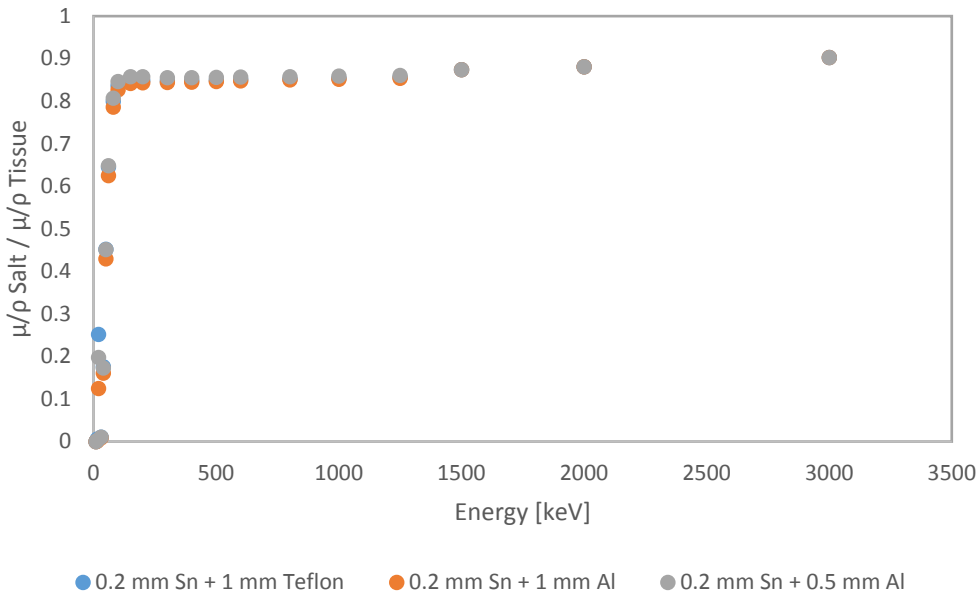

Figure 31. The same energy dependence ratio as in Figure 30 with added filter combinations to the salt. Three different filter combinations are presented.

As seen in Figure 31, three combinations of filters were added to the salt before the energy dependence was calculated. Applying a filter that evens out the response at low energies but do not change the response at higher energies is difficult. The idea in Figure 31 is to attenuate as much as possible the low energy photons and then create a small hole in the filter that will let in some known fraction of the low energy photons, unfiltered, to be registered by the salt detector.

4 Conclusions

- The optimal NaCl pellet is produced when using a compression force of about 3.0 tons and grain sizes between 100-400 μm. The dosimetric properties of the NaCl pellets show that they are suitable for dosimetry. The dose response is linear up to at least 6 Gy and dose estimations are possible up to 100 mGy, using a calibration dose of the same size as the unknown dose, i.e. for known salts dose determinations are possible up to at least 6 Gy whereas dose determinations from unknown salts are possible up to 100 mGy (with sufficient accuracy).
- The signal fading need to be further investigated in order to understand the inverse fading which occurs after about 10 days.
- Several of the salts investigated have suitable dosimetric properties and are commercially available in Swedish supermarkets. Both Falksalt 3 and Jozo can be used for dosimetry, whereas Falksalt 2 and 4 should be further investigated in the future.

- Based on the results of the dosimetric property e.g. dose response, it can be concluded that the new readout protocol can be used in OSL measurements without introducing larger uncertainties compared to the standard readout protocol.
- The NaCl pellets are similar in size and shape to the most commonly used LiF chips which means that the NaCl pellet can be used in the same applications as LiF chips without any major adjustments.
- The low background signal (zero when pre-bleached) and MDD of the salt makes it possible to estimate absorbed doses from the natural background after only three days.
- A badge holder need to be produced with appropriate energy compensation filters for the NaCl to work as a proper dosimeter in exposure situations with photon energies below 300 keV.

5 References

Ainsbury, E.A., Bakhanova, E., Barquinero, J.F., Brai, M., Chumak, V., Correcher, V., Darroudi, F., Fattibene, P., Gruel, G., Guclu, I., Horn, S., Jaworska, A., Kulka, U., Lindholm, C., Lloyd, D., Longo, A., Marrale, M., Gil Monteiro, O., Oestreicher, U., Pajic, J., Rakic, B., Romm, H., Trompier, F., Veronese, I., Voisin, P., Vral, A., Whitehouse, C.A., Wieser, A., Woda, C., Wojcik, A., Rothkamm, K., 2010. Review of retrospective dosimetry techiques for external ionising radiation exposures. Radiat. Prot. Dosimetry 1–20. doi:10.1093/rpd/ncq499

Bernhardsson, C., Christiansson, M., Mattson, S., Rääf, C.L., 2009. Household salt as a retrospective dosemeter using optically stimulated luminescence. Radiat. Environ. Biophys. 21–28. doi:10.1007/s00411-008-0191-y

Bøtter-Jensen, L., Markey, B.G., Poolton, N.R.J., Jungner, H., 1996. Luminescence Properties of Porcelain Ceramics Relevant to Retrospective Radiation Dosimetry. Radiat. pro 65, 369–372.

Christiansson, M., 2014. Household salt as an emergency radiation dosemeter for retrospective dose assessments using optically stimulated luminescence. [Doctoral dissertation series (Lund University, Faculty of Medicine)]: [2014:27]. Malmö : Department of Clinical Sciences, Malmö, Lund University, 2014.

Christiansson, M., Bernhardsson, C., Geber-Bergstrand, T., Mattson, S., Rääf, C.L., 2014. Household salt for retrospective dose assessments using OSL : signal integrity and its dependence on containment , sample collection , and signal readout. Radiat. Environ. Biophys. 559–569. doi:10.1007/s00411-014-0544-7

Christiansson, M., Bernhardsson, C., Mattsson, S., Rääf, C.L., 2011. Using an optimised OSL Single-aliquot regenerative dose protocol for low-dose retrospective dosimetry on household salt. Radiat. Prot. Dosimetry 144, 584–587.

Currie, L.A., 1999. Detection and quantification limits: origins and historical overview. Anal. Chim. Acta 127–134.

Currie, L.A., 1968. Limits for qualitative detection and quantitative determination. Application to radiochemistry. Anal. Chem. 40, 586–593. doi:10.1021/ac60259a007

Godfrey-Smith, D.I., 1994. Thermal effects in the optically stimulated luminescence of quartz and mixed feldspars from sediments. J. Phys. D. Appl. Phys. 1737–1746.

Hubbell, J.H. and Seltzer, S.M., 2004. Tables of X-Ray Mass Attenuation Coefficients and Mass Energy-Absorption Coefficients (version 1.4). [WWW Document]. NIST. URL http://physics.nist.gov/xaamdi

Kortov, V., 2007. Materials for thermoluminescent dosimetry : Current status and future trends. Radiat. Meas. 42, 576–581. doi:10.1016/j.radmeas.2007.02.067

Kunii, Y., Suzuki, Y., Shiga, T., Yabe, H., Yasumura, S., Maeda, M., Niwa, S.I., Otsuru, A., Mashiko, H., Abe, M., 2016. Severe Psychological Distress of Evacuees in Evacuation Zone Caused by the Fukushima Daiichi Nuclear Power Plant Accident: The Fukushima Health Management Survey. PLoS One 11, 1–10. doi:10.1371/journal.pone.0158821

Mckeever, S.W.S., Moscovitch, M., 2003. On the advantages and disadvantages of optically stimulated luminescence dosimetry and thermoluminescence dosimetry. Radiat. Prot. Dosimetry 104, 263–270.

Murakami, M., Ono, K., Tsubokura, M., Nomura, S., Oikawa, T., Oka, T., Kami, M., Oki, T., 2015. Was the risk from nursing-home evacuation after the Fukushima accident higher than the radiation

risk? PLoS One 10, 1–17. doi:10.1371/journal.pone.0137906

Ramzaev, V., Bøtter-jensen, L., Thomsen, K.J., Andersson, K.G., Murray, A.S., 2008. An assessment of cumulative external doses from Chernobyl fallout for a forested area in Russia using the optically stimulated luminescence from quartz inclusions in bricks. J. Environ. Radioact. 99, 1154–1164. doi:10.1016/j.jenvrad.2008.01.014

Thomsen, K.J., 2004. Optically Stimulated Luminescence Techniques in Retrospective Dosimetry using Single Grains of Quartz extracted from Unheated Materials.

Yukihara, E.G., Mckeever, S.W.S., 2011. Optically Stimulated Luminescence.

Zhang, J.F., Yan, C., Zhou, L.P., 2005. Feasibility of optical dating using halite. J. Lumin. 114, 234–240. doi:10.1016/j.jlumin.2005.01.009

6 Appendix A

Making NaCl pellets

A B C

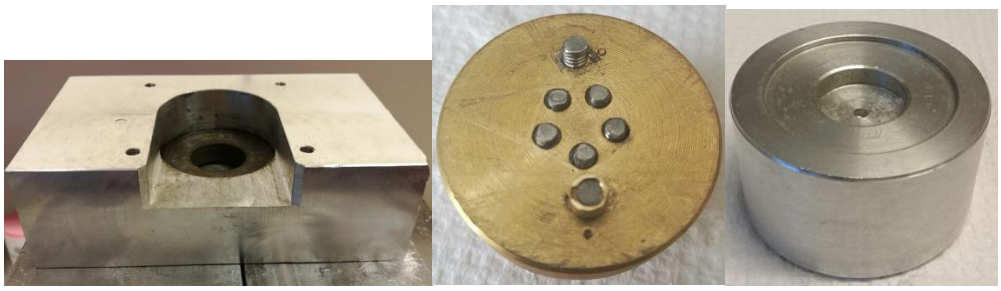

D E F

- Fill the 5 holes in part A of the instrument with salt. Remove excess salt.

- Put the top part (Part B) on part A and make sure the outer steering holes align.

- Put the parts, pressed together, in the stainless steel cup (Part C) and put the assembled tool in the press base, D, on top of the springs.

- Press to 2.5-3.0 Tons.
- Remove part B from part A
- Put part E on the backside of part A to push out the salt pellets. Make sure that the steering holes align.
- Put the parts in the higher cup, part F, and press until the rods in part A has been pushed out. Use the press.

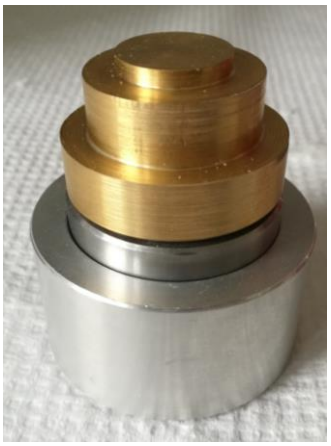

- Remove the pellets
- Restore the rods of part A to their original positions.

Appendix B

Figure 32 shows the signal decay curve when perofrming a readout after irradiation of Falksalt 3.

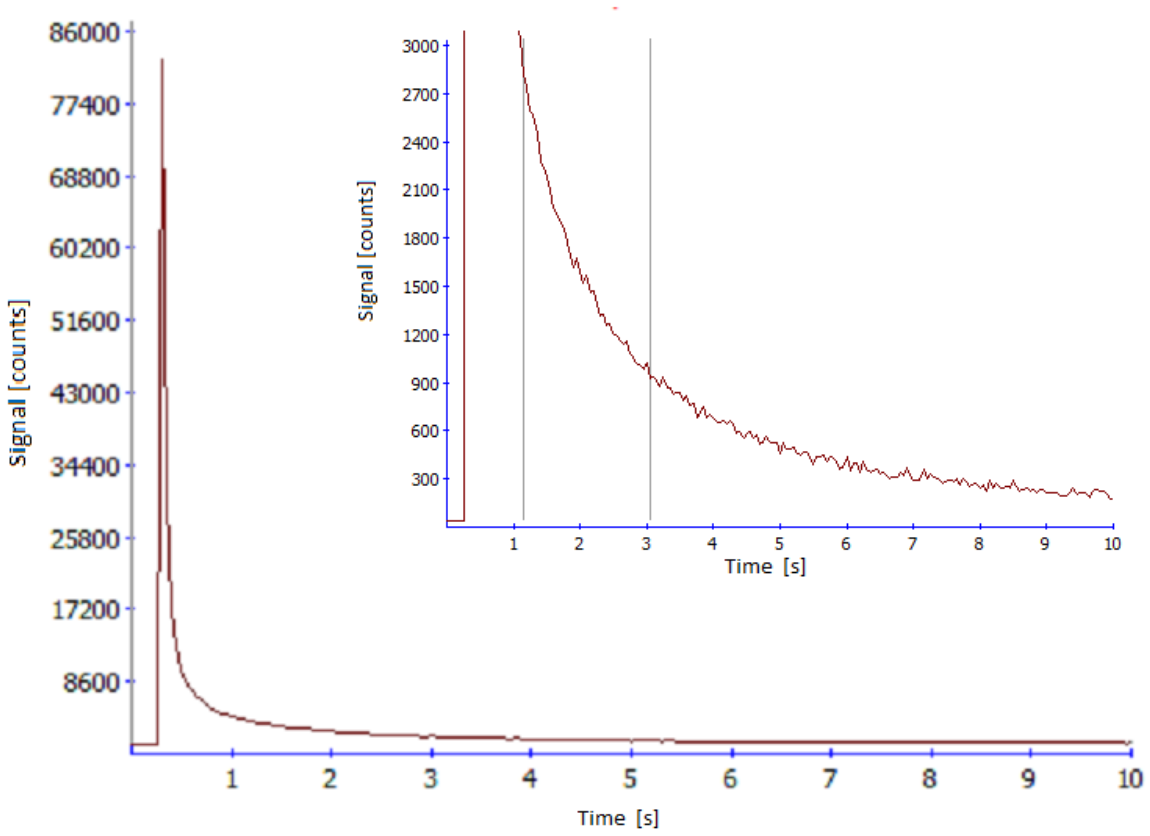

Figure 32: The figure shows the OSL signal decay curve when performing a signal readout after irradiation of Falksalt 3

Figure 33 shows the signal decay curve when perofrming a readout after irradiation of Falksalt 1.

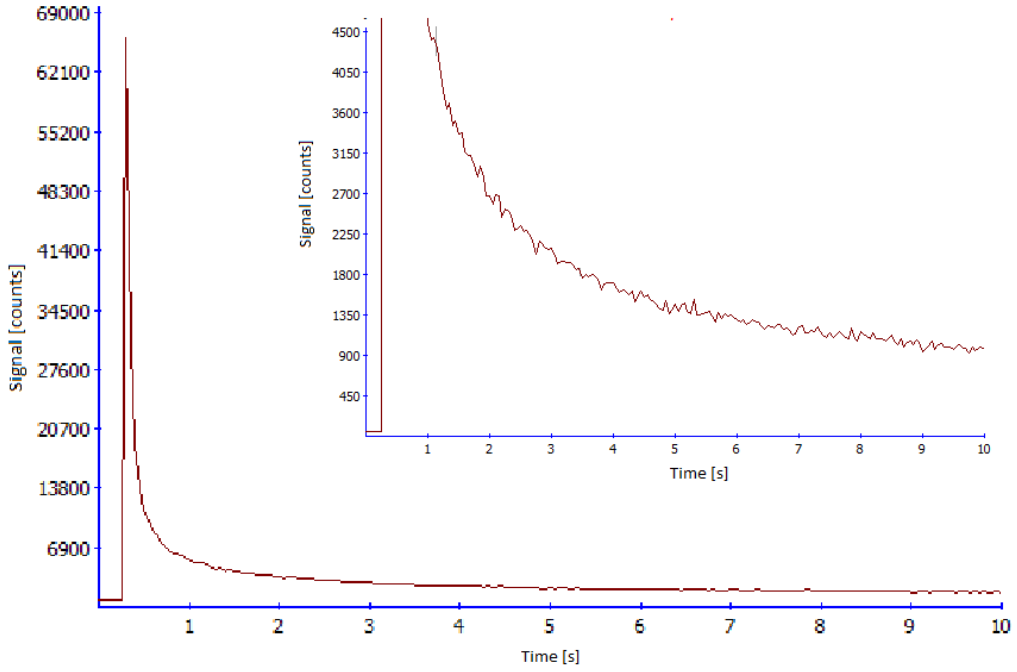

Figure 33: The figure shows the OSL signal decay curve curve when performing a signal readout after irradiation of Falksalt 1